European Journal of Medicinal Chemistry 226 (2021) 113805

Contents lists available at ScienceDirect

European Journal of Medicinal Chemistry

journal homepage: http://www.elsevier.com/locate/ejmech

Design, synthesis, and biological evaluation of novel pyrrolidinone small-molecule Formyl peptide receptor 2 agonists

Monika Maciuszek [a, b, *], Almudena Ortega-Gomez [c], Sanne L. Maas [c], Jose Garrido-Mesa [b], Bartolo Ferraro [c], Mauro Perretti [b], Andy Merritt [a], Gerry A.F. Nicolaes [f], Oliver Soehnlein [c, d, e], Timothy M. Chapman [a]

[a] LifeArc, Accelerator Building, Open Innovation Campus, Stevenage, UK
[b] The William Harvey Research Institute, Barts and the London School of Medicine, Queen Mary University of London, London, UK
[c] Institute for Cardiovascular Prevention (IPEK), LMU Munich Hospital, Munich, Germany
[d] Department of Physiology and Pharmacology (FyFa), Karolinska Institute, Stockholm, Sweden
[e] Institute for Experimental Pathology (ExPat), Centre for Molecular Biology of Inflammation, University of Münster, Münster, Germany
[f] CARIM – School for Cardiovascular Sciences Department of Biochemistry, Maastricht University, Maastricht, Netherlands

ARTICLE INFO

Article history:
Received 9 April 2021
Received in revised form
23 August 2021
Accepted 24 August 2021
Available online 2 September 2021

Keywords:
FPR2
Pharmacophore
Agonists
Neutrophils
Resolution of inflammation

ABSTRACT

A series of Formyl peptide receptor 2 small molecule agonists with a pyrrolidinone scaffold, derived from a combination of pharmacophore modelling and docking studies, were designed and synthesized. The GLASS (GPCR-Ligand Association) database was screened using a pharmacophore model. The most promising novel ligand structures were chosen and then tested in cellular assays (calcium mobilization and β-arrestin assays). Amongst the selected ligands, two pyrrolidinone compounds (**7** and **8**) turned out to be the most active. Moreover compound **7** was able to reduce the number of adherent neutrophils in a human neutrophil static adhesion assay which indicates its anti-inflammatory and proresolving properties. Further exploration and optimization of new ligands showed that heterocyclic rings, e.g. pyrazole directly connected to the pyrrolidinone scaffold, provide good stability and a boost in the agonistic activity. The compounds of most interest (**7** and **30**) were tested in an ERK phosphorylation assay, demonstrating selectivity towards FPR2 over FPR1. Compound **7** was examined in an *in vivo* mouse pharmacokinetic study. Compound **7** may be a valuable *in vivo* tool and help improve understanding of the role of the FPR2 receptor in the resolution of inflammation process.

1. Introduction

Chronic inflammation has a crucial role in the development of many cardiovascular diseases such as atherosclerosis [1], myocardial ischaemia–reperfusion [2–4] and thrombosis [5]. In general, desirable physiological inflammation is a response of our immune system to harmful stimuli and it is contained in time and space. However prolonged and unresolved inflammatory response leads to chronic inflammation. Resolution-based treatments can reduce harmful effects, enhancing the self-recovery abilities of tissues and assisting the return of homeostasis. One of the most studied pro-resolving receptors is Formyl peptide receptor 2 (FPR2), a member of the protein family of G protein-coupled receptors (GPCRs), abundantly expressed in neutrophils [6–10], monocytes [11,12], epithelia, endothelia, smooth muscle cells [1], and fibroblasts. FPR2 exhibits numerous physiological and pharmacological responses and can be activated by ligands of diverse origins such as peptides, lipids and small molecules [13–16]. The receptor has a dual impact on the inflammatory response which varies depending on the nature of the ligand [17]. FPR2 can be activated by agonists like annexin A1 or LXA_4 to resolve the inflammation. These types of agonists promote apoptosis of neutrophils, macrophage-mediated phagocytosis, and inhibition of epithelial activation as a mechanism of resolving acute inflammatory responses. In contrast, the FPR2 receptor may be activated by proinflammatory molecules such as Serum amyloid A (SAA), LL-37 (the cleaved antimicrobial peptide from Cathelicidin) and mitochondrial hexapeptides and trigger the transmigration and survival of neutrophils, epithelial

* Corresponding author. LifeArc, Accelerator Building, Open Innovation Campus, Stevenage, UK.
E-mail address: maciuszekmonika@gmail.com (M. Maciuszek).

https://doi.org/10.1016/j.ejmech.2021.113805
0223-5234/

activation and monocytes recruitment [18]. Since 2004 research groups have concentrated on the proresolving properties of the FPR2 receptor and several synthetic small molecules have been submitted for Phase I clinical trials [19,20], but none of them have yet moved beyond this. Nevertheless, FPR2 is one of the key targets in the resolution of inflammation [14,21,22]. In this work, we present a novel pyrrolidinone series, where the first stage was to develop pharmacophore models and to investigate a homology model obtained from GPCRdb [23,24] for molecular docking; these were then used in the structure-based pursuit of novel agonists. To discover novel FPR2 agonist structures we screened the GLASS (GPCR-Ligand Association) database. Each compound was evaluated for its agonistic activity to stimulate calcium mobilization and β-arrestin recruitment in CHO−K1 FPRL1 cells (DISCOVERx) overexpressing hFPR2. The PathHunter™ GPCR β-Arrestin assay was applied in our studies to test the ligands' ability to activate the β-arrestin signalling cascade [25]. Ligand-induced β-arrestin recruitment is involved in numerous processes such as kinase activation, desensitization, and receptor internalization [26]. Upon activation of the GPCR, if the receptor couples to Gαq, it produces an increase in intracellular Ca^{2+}. In these studies, the increase in cytosolic Ca^{2+} was measured by the FLIPR® Tetra® High-Throughput Cellular Screening System [27]. The increase in levels of intracellular Ca^{2+} is initiated by the activation of phospholipase C enzymes and a boost in protein kinase C (PKC) production is observed [28]. FPR2 activation is initiated by binding of the ligand from the extracellular side and classic agonists have been perceived as ligands with the ability to trigger numerous signalling pathways downstream of a receptor [29]. However, depending on the nature of the ligand, the G protein or β-arrestin signalling can be independently activated, or the ligand can simultaneously trigger both pathways [30,31]. Therefore, we considered it worthwhile to use both of these assays, where we can monitor activation of two different pathways. The knowledge gained from these two distinctive assays can bring an insight into whether we have full or biased agonists. Moreover, both assays are convenient for high throughput screening, because of their robustness and reproducibility. Compounds were also tested in *in vitro* absorption, distribution, metabolism and excretion and toxicity (ADMET) assays to bring greater understanding to their potential for further development. Two lead compounds with the best profiles (**7** and **30**) were then tested in an ERK phosphorylation assay (FPR1 and FPR2 HEK cell lines). The activation of ERK signalling in cardiomyocytes promotes beneficial and prosurvival effects [32−34]. Finally, compound **7** was tested in an *in vivo* mouse pharmacokinetic study, which demonstrated its potential for use as an *in vivo* tool.

2. Results and discussion

2.1. In silico studies

In order to discover novel FPR2 agonists we decided to use the GLASS (GPCR-Ligand Association) database [35] which is a repository for experimentally validated GPCR-ligand interactions. The workflow is summarised in Fig. 1. A: as a first stage we excluded possible duplicates and structures which do not meet the Lipinski rule of 5 using Pipeline Pilot. The next step was the generation of 3D conformers of all molecules in the GLASS-db employing the Ligprep tool (Schrödinger software). Then the compounds were screened using a five-point pharmacophore model ADHHR_7 previously described by our group [36]. The ADHHR_7 pharmacophore model was developed (Fig. 2) employing the Phase tool in Schrödinger Maestro [37]. The examples of FPR2 small molecule agonists used in pharmacophore studies were included in the supporting information. Because of the heterogeneity among the examined agonists,

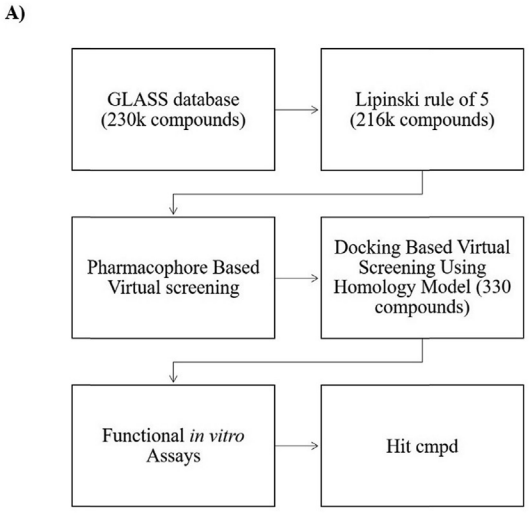

		7	8
R		H	-F
Kinetic solubility [μM]		15	0
Intrinsic Clearance (CL_{int}) [μL/min/mg protein]	HLM	2.2	2.8
	MLM	2	46
Half Life ($T_{1/2}$) [min]	HLM	> 400	> 400
	MLM	>400	33
LogD		>4	>4
β-arrestin EC_{50} [nM]		302	510
Calcium mobilization EC_{50} [nM]		310	7000

Fig. 1. A) Selection of the compounds using Phase Ligand screening B) Hit compounds and their characterization; Ks and LogD were measured at pH 7.4.

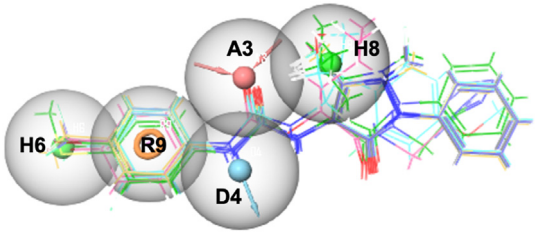

Fig. 2. Five point pharmacophore model of FPR2 agonists. H-hydrophobic R-ring; D-hydrogen bond donating and A - accepting sites in the receptor.

the pharmacophore model was established using the 'multiple ligands' option with the method 'best alignment and common features' A shortlist of 330 compounds was selected based on the results of pharmacophore screening. In the next stage these ligands were docked into the FPR2 receptor homology model with the aim of assessing their potential binding poses. Glide SP-protocol was selected, and all ligands were treated as flexible molecules. The docking poses were manually analysed for their interactions with key amino-acid residues such as His-102, Arg-205, Cys-176, Phe-257, Phe-292, Phe-163 and Tyr-175. From this, a set of 13 novel

ligands was selected and functionally tested. Amongst these ligands, two pyrrolidinone compounds were the most promising, the compounds **7** and **8** showed nanomolar agonistic activity in β-arrestin (EC_{50} = 302 nM and 510 nM respectively). However, in calcium mobilization the 4-fluoro analogue **8** exhibited a distinct drop-off in the potency compared **7** (Fig. 1B).

2.2. Design and development of pyrrolidinone FPR2 agonists

Compound **7** was selected for further optimization based on the outcomes of the cellular assays and in-house *in vitro* ADME assays. The stability of the compound was determined in human and mouse liver microsomes, where it was extremely stable ($T_{1/2}$ >400 min). In addition, the hit compounds did not show a cytotoxic effect in a cell health assay (**supporting information**). The low kinetic solubility and high logD value of compound **7** were two properties to be improved, while preserving or increasing the agonistic activity (Fig. 1 B). Furthermore, encouraging results from human neutrophil adhesion assays were an additional factor which fed into the selection of compound **7** for further optimization. Fig. 3 shows the results obtained from a known active FPR2 agonist and novel pyrrolidinone compound **7**. Compound **A**, which is one of the Allergan small molecule agonists described in patent application US20170320897 covering the treatment of ocular inflammation, showed significant inhibition of neutrophil adhesion in the μM range (Fig. 3). Similarly, compound **7** decreased the number of adherent neutrophils in a concentration-dependent manner with a significant reduction from 10 μM onwards, hence revealing promising anti-inflammatory properties [38–40].

In the next step of compound optimization, around 2000 virtual compounds were proposed in which the phenyl ring attached to the pyrrolidinone core was replaced, and their predicted binding to the homology model was examined after docking using Schrödinger software. The docking studies suggested that molecules that resemble **7** (blue) are likely to occupy subpockets I and II, whereas compounds containing an additional linker attached to the pyrrolidinone core such as **16** (pink) and **15** (green) can potentially bind into subpockets III and I with formation of hydrogen bonds with amino-acid residues such as Cys-176 and His-102 (Fig. 4).

With the introduction of the linkers to the pyrrolidinone core, we could obtain improved ligand fitting as well as enhanced three-dimensionality in the structures. A variety of linkers was proposed including alkyl moieties and ring features, for example: piperidine, pyrrolidine, azetidine, and heterocyclic aromatic rings such as pyrazoles and oxadiazoles. In Table 1, the first structural modifications of compound **7** are presented. The benzyl analogue compound **9** unexpectedly showed no activity in both functional assays. However, it did show improved solubility and good microsomal stability across two species. The additional synthesized compounds **10**–**21** in Table 1 contain heterocycles such as piperidine, pyrrolidine, azetidine, and pyrazole, and were designed to increase the polarity and aqueous solubility of the molecules. Compounds **15** and **16** showed well balanced profiles with respect to activity and properties and both contain a piperidine ring as a linker group; the piperidine ring is a frequent motif in numerous natural alkaloids and synthetic small molecules. The introduction of the benzyl moiety in compound **16** allowed us to maintain the basic nitrogen of piperidine, which resulted in good kinetic solubility (Ks = 152 μM). An additional $-CH_2$ moiety between the pyrrolidinone core and piperidine linker (compound **15**), led to a decrease of one unit in LogD compared to **16** and a decrease in microsomal clearance of around 2-fold in both HLM and MLM. Replacement of the piperidine linker with pyrrolidine produced another stereo centre in the molecule which resulted in two diastereoisomers **17** and **18**, which displayed inferior microsomal stabilities relative to

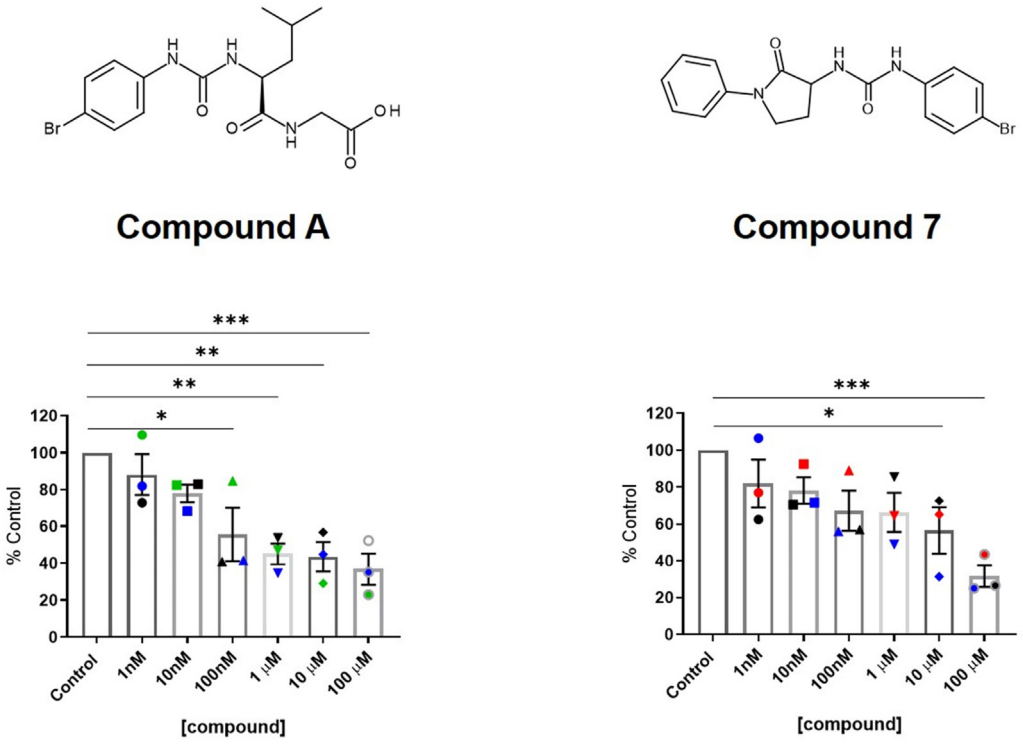

Fig. 3. Anti-adhesive properties of FPR2 agonists A and 7 in a human neutrophil static adhesion assay. Data are depicted as mean, with 3 independent experiments and 3 technical replicates; The differences between the control group, and treatment groups were evaluated by one-way ANOVA followed by Dunnett's multiple comparison test, and the differences were considered significant for a P value < 0.05: *P < 0.05, **P < 0.01, ***P < 0.001; ns – not significant.

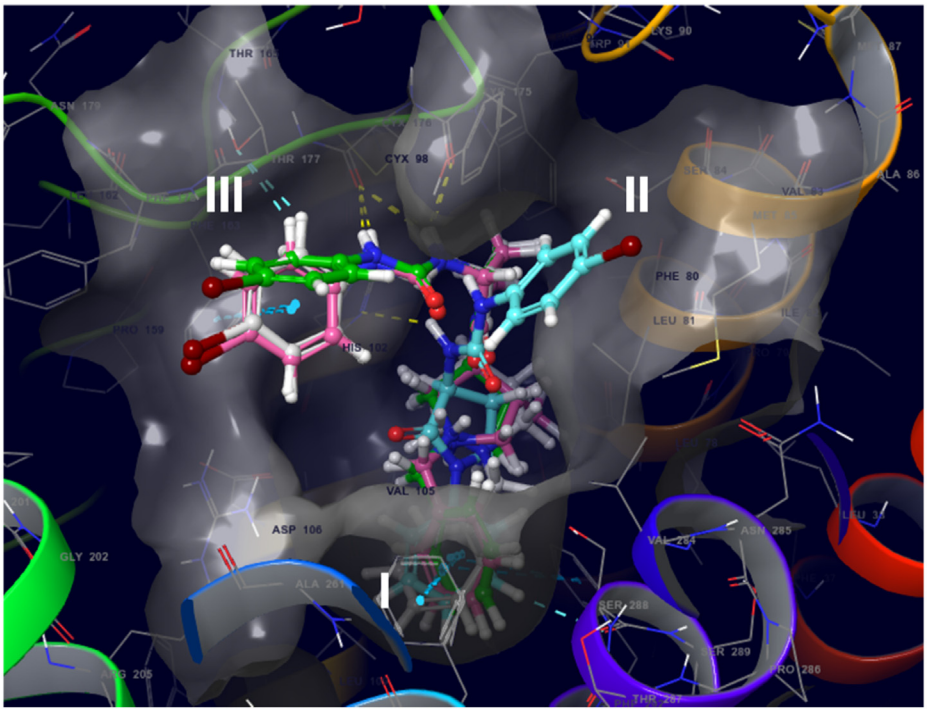

Fig. 4. Binding poses of pyrrolidinone agonists. Compound **7** (blue) occupies subpockets I and II where compounds **16** (pink), **15** (green), and (grey) occupy subpockets I and III.

15 and **16.** Compounds **19** and **20**, with a 3-piperidine linker, also showed higher microsomal clearance. Compound **21** with a 3,5-dimethyl-pyrazole linker displays acceptable stability in HLM, although poorer stability in MLM. It exhibited full activation in both functional assays in the nanomolar range with a promising ADME profile, although the LogD requires improvement. The last ligand described in Table 1 is compound **22**, in this case we replaced the benzyl ring with pyrimidine. It displayed a good activity profile in both cellular assays (Calcium EC_{50} = 0.008 μM and β-arrestin EC_{50} = 0.385 μM). However, the logD value increased by a half log unit and the solubility was lost. The introduction of pyrimidine did not improve the microsomal stability, which might indicate a possible metabolic hotspot. Across these new compounds, we observed good metabolic stability *in vitro* and activity in the nanomolar range, yet the agonistic SAR is relatively flat (see Table 2).

In the second phase of structural optimization, we focused on the evaluation of the *para*-bromo-phenylureidic part of compound **7**. Seven novel compounds were proposed: four replacements of the *para*-bromo moiety with −CN (**29**), -Et (**25**), $-OCH_3$ (**27**) or 3,5-difluoro substituents (**26**), and three alternatives for the phenyl ring: imidazole (**23**) and two 4-pyridine containing analogues (**24** and **28**). Based on docking studies, we decided to introduce two compounds with a small modification on the core. Ligands **23** and **28** contain the extra methyl group in the pyrrolidinone core showed plausible binding poses. The results from *in silico* SAR studies were used to guide these modifications. Docking studies suggested that in the case of compounds **29** (grey) and **24** (pink), the phenyl ring connected directly to the pyrrolidinone core is located in the deepest pocket I, created by hydrophobic amino acid residues such as Phe-292, Phe-257. An aromatic ring attached to the urea moiety forms the aromatic π-stacking interaction with Tyr-175. The NH groups of the urea moiety act as hydrogen bond donors and interact with Cys-176 and His-102. Moreover, *in silico* studies showed a possible second binding mode represented by the compounds **26** (orange) and **25** (blue). These ligands contain a pyrazole moiety which is linked directly to pyrrolidinone core. In these examples, a flip into the subpocket II is observed. This subpocket is built with amino acid residues for example Ser 84, Val 284, Tyr 175. The imidazole ring is not buried in the subpocket I but occupies the subpocket II, making a π-π interaction with the phenyl ring of Tyr-175 sidechain. Finally, the NH groups of the urea moiety act as hydrogen bond donors and interact with hydroxy groups of Ser-288 located in second polar cluster (Fig. 5).

Amongst compounds **23**–**29**, only **29** showed a hint of agonistic activity in the calcium mobilization assay. This might be explained by the fact that **29** is the only molecule where the phenyl ring is attached directly to the urea group. This makes the molecule less flexible and perhaps it is responsible for better fitting in the binding pocket. The lack of activity could be triggered also by poor solubility of the molecules.

Having demonstrated that an additional linker helps the compound fit better into sub-pocket I of the FPR2 binding site and improves the solubility while maintaining good agonistic potency, our efforts moved to further optimizing the linkers. Based on the information gained from the ADME and functional assays, molecule **21** was chosen for further modification. Four additional analogues were synthesized and tested (Table 3). Ligands **30**–**33** were designed to explore the effect of varying substitution pattern around the pyrazole. Compounds **32**–**33** lack activity in the calcium mobilization assay. The conformational twist induced by the 3,5-dimethyl group in **21** may in itself be beneficial for potency, but it can also aid solubility, which could be a limiting factor in **32** and **33**. The dimethyl substituted example **30** compared to **21**, showed increased microsomal stability including both species and gave a good LogD value (2.6). The introduction of dimethylpyrazole resulted in a 1.5-fold decrease (EC_{50} = 0.740 μM) in β-arrestin recruitment but it improved the calcium mobilization (EC_{50} = 0.142 μM) activity by 2-fold compared with **21**. For compound **31**, the isopropyl moiety enhanced the microsomal stability and lowered the LogD value, however **31** exhibits 3-fold decrease in the calcium mobilization assay (EC_{50} = 0.884 μM) compared to the

Table 1
ADME properties and EC_{50} values for pyrrolidinone derivatives.

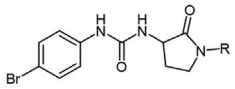

ID	R	KS [μM]	LogD	Microsomal stability				Ca^{2+} EC_{50} [μM] (E_{max})	β arrestin EC_{50} [μM] (E_{max})
				$T_{½}$ [min]		CLint (μL/min/mg)			
				HLM	MLM	HLM	MLM		
7		15	>4	>400	>400	2	2	0.43 (73)	0.30
8	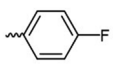	0	>4	>400	33	3	46	1.97	0.51
9		75	4.4	168	127	9	12	N.A.	N.A.
10	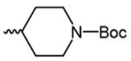	61	4.6	250	31.3	6	49	0.73 (42)	6.3 (93)
11	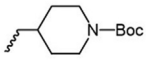	43	>4	19	19	80	80	0.40 (86)	2.16 (92)
12	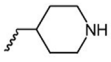	227	0.8	381	140	4	11	0.27 (84)	3.29 (102)
13	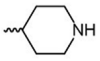	234	0.3	–	–	<2	<2	0.23 (68)	1.03 (100)
14	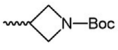	222	>4	113	112	14	14	0.41 (67)	2.35 (103)
15	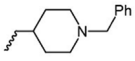	192	2.5	227	121	7	12	0.25 (99)	2.25 (93)
16	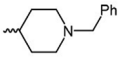	152	3.5	112	70	13	21	0.35 (76)	2.87 (96)
17 diastereomer I	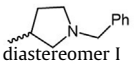	210	3.3	78	35	20	44	2.7 (128)	1.37 (100)
18 diastereomer II	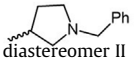	207	3.0	56	36	28	43	0.37 (84)	0.70 (99)
19 diastereomer I		71	>4	35	19	44	80	0.13 (71)	1.38 (89)
20 diastereomer II		54	4.1	71	30	22	50	0.06 (73)	0.55 (86)
21		57	4.6	189	38	8	40	0.28 (150)	0.40 (95)
22	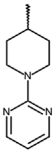	0	3.9	57	44	27	35	0.008	0.385 (96)

N.A. - very low response (E_{max} <20% of max response) or weak activation EC_{50} > 10 μM; Ks and LogD were measured at pH 7.4.

Table 2
The replacement of phenylureidic group in pyrrolidinone series.

Compound	LogD	Microsomal stability				Ca^{2+} EC_{50} [μM]	β arrestin EC_{50} [μM]
		$T_{1/2}$[min]		Clint (mL/min/mg)			
		HLM	MLM	HLM	MLM		
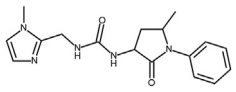 23	1.0	–	–	<2	<2	N.A.	N.A.
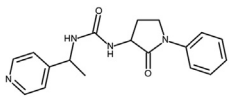 24	2.0	410		3.8	<2	N.A.	N.A.
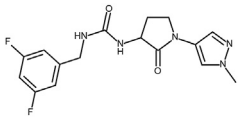 25	2.1	584		2.6	<2	N.A.	N.A.
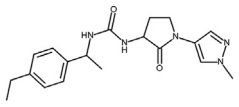 26	not tested	not tested		not tested		N.A.	N.A.
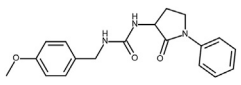 27	2.8	329	357	4.7	4.3	N.A.	N.A.
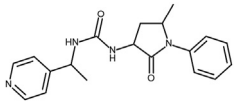 28	1.99	505	151	3.0	10.2	N.A.	N.A.
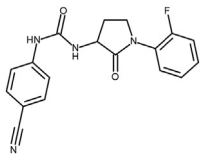 29	2.7	85	172	17.94	8.9	15 (123)	N.A.

N.A. - very low response (E_{max} <30% of max response) or weak activation EC_{50} > 10 μM; Ks and LogD were measured at pH 7.4.

lead compound **21;** this can be explained by the lack of a methyl group and its insolubility (see Table 4).

2.3. Chemistry

The synthesis of the pyrrolidine series was started with N-acylation of the desired amine with **34** resulting in formation of N-substituted 2,4-dibromo-butanamide intermediate. The crude product was used without any further purification in the cyclization (**35**–**50**). Total yield after two steps was in the range 30–60%. The introduction of the amine group is performed by stirring the substrate in a mixture of acetonitrile: aqueous ammonia 1:1 at 40 °C overnight to form products **51**–**65** in good yield. The urea derivatives were obtained by reacting intermediates with 4-bromophenyl isocyanate at ambient temperature overnight (**9**–**11, 14, 19**–**22, 30**–**33, 66**–**67**). Removal of the BOC protecting group was performed with 4 M HCl in dioxane at room temperature to obtain the products as free bases in quantitative yield using SPE cartridges (**12**–**13, 68**–**69**). *N*-alkylation, employing classic conditions with Hünig's base and benzyl bromide, yielded the final compounds **15**–**18** (Scheme 1).

2.4. The ERK phosphorylation assay

The two lead compounds (**7** and **30**) were tested in an ERK Phosphorylation Assay, using W peptide as a positive control. To this end, we used HEK cells stably transfected with human FPR1 or FPR2 [41], on the notion that activation of ERK phosphorylation is a tissue-protective proresolving signalling, as demonstrated for pro-survival effects in cardiomyocytes [32-34], [42]. At this stage we wanted to investigate the selective agonistic activity of the pyrrolidinone series and elucidate whether the proresolving strategy will contribute to regulate human inflammatory diseases and their implications. When tested in a concentration-response manner, ranging from 1 nM to 30 μM, both FPR agonists did not show any significant effects in hFPR1-HEK cells, demonstrating their lack of functional responses at FPR1. In contrast a positive stimulation of ERK phosphorylation was observed in FPR2 HEK cells, with calculated EC_{50} of 7.36 and 4.88 μM, for compounds **7** and **30** respectively. The normal mock-transfected HEK cell line was used as a control in order to examine any possible off-target effects of the compounds. No off-target effect was observed (**supporting information**).

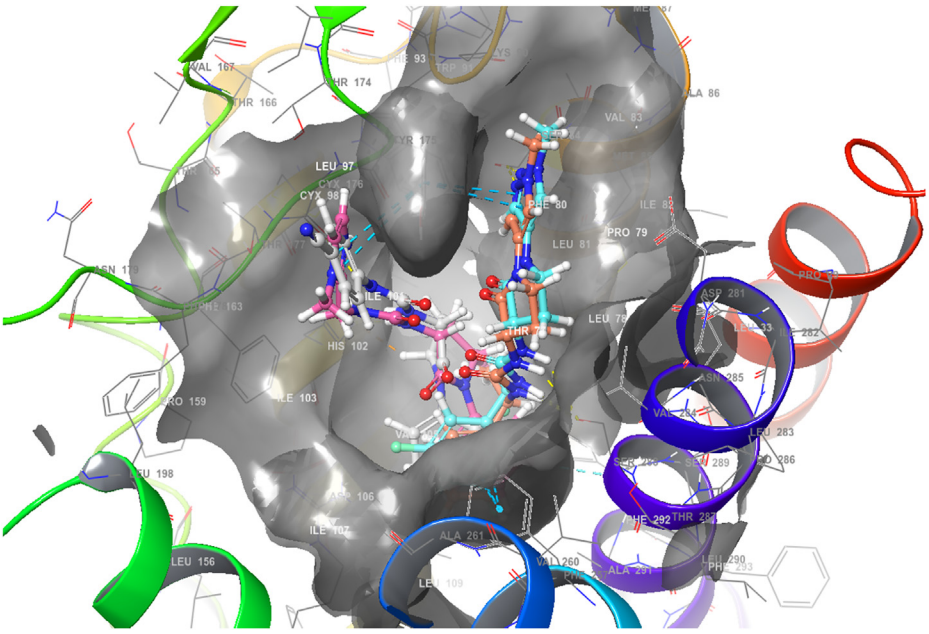

Fig. 5. Proposed binding modes for non-*para*-bromo-phenylureidic pyrrolidinone analogues: **29** (grey), **24** (pink), **26** (orange) and **25** (blue).

Table 3
The additional analogues of pyrrolidinone series.

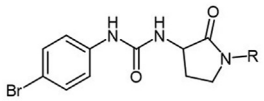

ID	R	Ks [μM]	LogD	Microsomal stability				Ca^{2+} EC_{50} [μM] (E_{max})	β-arrestin EC_{50} [μM] (E_{max})
				$T_{1/2}$ [min]		Clint (mL/min/mg)			
				HLM	MLM	HLM	MLM		
30	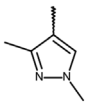	9	2.6	183	172	8	9	0.142	0.74 (98)
31	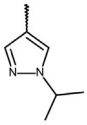	1	3.7	322	159.3	526	10	0.884	NA
32	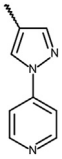	3	4.3	658		2		N.A.	3.76 (103)
33	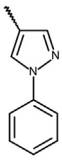	0	>4	209	107	7	14	N.A.	N.A.

N.A. - very low response (E_{max} <30% of max response) or weak activation EC_{50} > 10 μM, Ks and LogD were measured at pH 7.4.

2.5. PK studies

Compound **7** was chosen for pharmacokinetic studies which were performed in male C57BL6 mice with intraperitoneal administration at 10 mg/kg. Following a single IP dose, compound **7** was rapidly absorbed (T_{max} = 0.25 h) and showed a good C_{max} and half-life (9.42 h) along with high exposure (Table 5).

Table 4
ERK phosphorylation assay.

Compound	FPR1 HEK		FPR2 HEK	
	E_{max}[a]	EC_{50} (μM)	E_{max}[a]	EC_{50} (μM)
7	*15*	*1.74*	*69*	*7.36*
30	*N.A.*	*N.A.*	90	4.88
W peptide	100	0.28	100	0.008

[a] E_{max} is described as percentage of Emax obtained from W peptide (3 μM), N.A. - not active/very weak.

3. Conclusions

In summary, our goal was to identify, develop and synthesize novel FPR2 small molecule agonists, using a 'ready-to-use' homology model, molecular docking, and pharmacophore modelling studies. Over 210,000 ligands were screened from the GLASS database using our pharmacophore model. Thirteen selected ligands were tested in the functional assays to examine their agonistic activity. The initial hit compounds **7** and **8** with a pyrrolidinone core were identified. Compound **7** displayed nanomolar activity (β-arrestin EC_{50} = 302 nM, Calcium mobilization EC_{50} = 430 nM); its 4-fluoro analogue **8** showed only a minor drop-off in the β-arrestin recruitment assay (EC_{50} = 510 nM), but a significant decrease in potency in calcium mobilization. Moreover, promising results from human neutrophil adhesion assays demonstrated the anti-inflammatory properties of compound **7**. Further optimization was then carried out, the first round of which involved the introduction of a range of linkers. This showed that increased polarity and increased sp [3]-character was tolerated and resulted in compounds with lower log D and enhanced solubility, such as the piperidines **15** and **16**. Also notably the dimethylpyrazole compound **21** displayed a promising ADME profile and maintained activity in the nanomolar range. The compounds exhibited no cytotoxic effects in a cell health assay. Further optimization focused on the evaluation of the *para*-bromo-phenyl-ureidic part of compound **7**, but changes in this region were not well tolerated. The final round of investigation confirmed that heterocyclic rings such as pyrazole directly attached to the pyrrolidinone core gave rise to good stability and increase of potency (**30**). Finally, two lead compounds **7** and **30** were tested in an ERK Phosphorylation Assay which demonstrated their lack of functional responses at FPR1, and selectivity towards FPR2. Moreover compound **7** showed a promising pharmacokinetic profile during intraperitoneal administration at 10 mg/kg in male C57BL6 mice. For future work, we would like to perform chiral separation of the lead compounds and test the two enantiomers in the cellular assays, to reveal the preference in the chirality of the molecules in terms of receptor activation and their ADME profiles.

4. Materials and methods

4.1. In silico studies

4.1.1. Homology model

An agonist bound μ-opioid based receptor structure was obtained from GPCRDB [http://gpcrdb.org/protein/fpr2_human/] Full protein sequence alignment can be found in the supporting information [23,24].

4.1.2. Docking studies

Protein-Ligand docking was performed using the Glide SP-protocol. All ligands were treated as flexible molecules. Binding site was identified using by Sitemap (Schrödinger Release 2018−2: Schrödinger, LLC, New York, 2018.) Ligands were prepared and visualized using Maestro 11.5. To generate decoys for active agonists DUDE database (http://dude.docking.org/) was used. The collection of compounds was implemented in Pipeline Pilot to eliminate possible duplicates and compounds which do not meet the Lipinski rule of 5 (Pipeline Pilot BIOVIA, Dassault Systèmes, San Diego, 2018.)

4.1.3. Pharmacophore studies

Pharmacophore hypothesis was obtained from multiple active ligands using Phase (Schrödinger Release 2018−2: Schrödinger, LLC, New York, 2018).

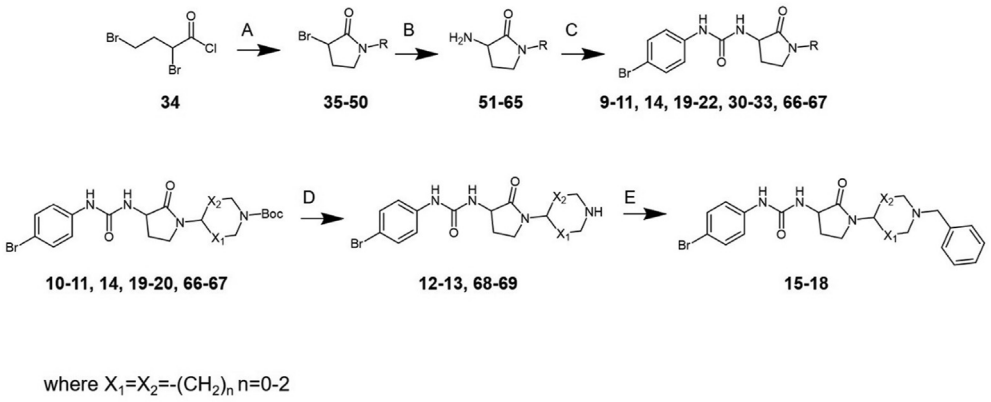

Scheme 1. Synthetic pathway for pyrrolidinone series.
Conditions: **A)** 1) 2 eq. TEA, 1 eq. amine, Et_2O or THF, 0 °C to RT, overnight; 2) 1.5 eq. sodium hydride (60 mass%) in mineral oil, THF, 0 °C to RT, 2−6 h; **B)** 35% aq. Ammonia/acetonitrile 1/1, 40 °C, overnight; **C)** 1.1 equiv. isocyanate, DCM/DMF 9/1, RT, overnight **D)** 4 M HCl in dioxane, DCM, 0 °C to RT; 2−4 h; **E)** 2.5 eq. DIPEA, 1.1eq. benzyl bromide, DMF, RT, overnight.

Table 5
In vivo mouse PK parameters for compound **7** with intraperitoneal administration.

Dose [mg/kg]	C_{max} [ng/mL]	T_{max} [h]	$T_{1/2}$ [h]	$AUC_{0\text{-last}}$ [ng·h/mL]	$AUC_{0\text{-inf}}$ [ng·h/mL]	AUC_{Extra} [%]	$MRT_{0\text{-last}}$ [h]
10	3608	0.25	9.42	28615	34968	18.17	9.20

4.2. Chemistry

All reagents were purchased from Sigma-Aldrich, Enamine, Fluorochem and other major suppliers and used without further purification. Solvents were purchased from Fisher Scientific (HPLC grade) or Sigma-Aldrich (anhydrous). Flash column chromatography was carried out with Biotage KP-Sil Snap cartridges using a Biotage Isolera-One and HPLC grade solvents. Reverse phase column chromatography was carried out on a Biotage Isolera with prepacked columns of C18 silica and HPLC grade solvents and buffers (Buffer A: 0.1% Ammonium Hydroxide in water; Buffer B: 0.1% Trifluoroacetic acid in water). Purification of compounds by preparative HPLC was carried out on an Agilent Reverse Phase Mass Directed Prep HPLC system by a member of the purification team. LC-MS was carried out on an Agilent 6120 quadrupole LC-MS with an Xbridge C18 column (3.5 μm particle and 4.6 × 30 mm dimension) and a diode array UV detector. Four methods were used depending on the nature of the compound: Method A: flow rate: 3 mL/min; Run time: 3.2 min: Solvent A: 0.1% Trifluoro Acetic acid in water, Solvent B: Acetonitrile; Gradient - 10–100%B; Gradient time: 2.35 min; Method B: flow rate: 3 mL/min; Run time: 3.2 min: Solvent A: 0.1% Ammonium Hydroxide in water, Solvent B: Acetonitrile; Gradient - 10–100%B; Gradient time: 2.35min; Method C: flow rate: 3 mL/min; Run time: 3.2 min: Solvent A: 0.1% Trifluoro Acetic acid in water, Solvent B: Methanol; Gradient - 10–100%B; Gradient time: 2.35min; Method D: flow rate: 3 mL/min; Run time: 3.2 min: Solvent A: 0.1% Ammonium Hydroxide in water, Solvent B: Methanol; Gradient - 10–100%B; Gradient time: 2.35min. HRMS were recorded on a Thermo-Fisher Q-Exactive operating at 70,000 Resolution. NMR solvents were obtained from Cambridge Isotope Labs. All ^{1}H NMR (500 MHz) and ^{13}C NMR (126 MHz) spectra were recorded on a JEOL ECA-500 spectrometer at 21 °C. Chemical shifts (δ) are in ppm and are relative to residual undeuterated NMR solvent. Spectra are referenced to a singlet at 7.27 ppm ($CDCl_3$), the centreline of quintet at 2.50 ppm ($(CD_3)_2SO$), quintet at 3.31 ppm (CD_3OD) for ^{1}H NMR and to the centreline of a triplet at 77.23 ppm ($CDCl_3$), septet at 39.7 ppm ($(CD_3)_2SO$), septet at 49.15 ppm (CD_3OD) for ^{13}C NMR. All ^{13}C NMR spectra were proton decoupled.

4.2.1. General procedure A for amide formation from acyl chloride and cyclization of pyrrolidinone

To a solution of amine (1 equiv.) in anhydrous diethyl ether (12 mL) was added, under inert atmosphere, triethylamine (2 equiv.) followed by a 2,4-dibromobutanoyl chloride (1.1 equiv.). After 16 h at room temperature, the solution was filtered, and the filtrate concentrated under reduced pressure. The solvent was evaporated, and the crude product was used in the next step without further purification. A sodium hydride (60 mass%) in mineral oil (1.2–1.5 equiv.) was added to a stirred solution of intermediate (1 equiv.) in tetrahydrofuran at 0 °C. The reaction mixture was allowed to warm up to room temperature and stir for an additional 2 h. The reaction was carefully quenched with ice and diluted with water. The resulting mixture was extracted with EtOAc. The combined organic layers were washed with brine and water. The organic phase was filtered through a phase separator and concentrated under reduced pressure. Crude product was dry loaded on silica and purified by flash column chromatography to obtain desired product.

4.2.1.1. 1-Benzyl-3-bromo-pyrrolidin-2-one (35). Prepared according to general procedure A with phenylmethanamine (0.93 mmol). and 2,4-dibromobutanoyl chloride (1.2 equiv., 1.12 mmol). Crude product was dry loaded on silica and purified by flash column chromatography (25 g silica gel, PE/EA 0→70% 15CV gradient) to obtain desired product. Yield: 200 mg, 75%; Appearance: yellow oil; LCMS: 1.78 min, *m/z* 254.0, 256.1 ($(M + H)^+$ 1:1, $^{79/81}$Br, ^{1}H NMR (500 MHz, $CDCl_3$) δ ppm 7.38–7.26 (m, 4 H), 7.25–7.23 (m, 1 H), 4.57–4.52 (m, 1 H), 4.47 (dd, J = 7.45, 2.29 Hz, 1 H), 4.46–4.41 (m, 1 H), 3.46–3.38 (m, 1 H), 3.20 (ddd, J = 9.88, 7.88, 2.29 Hz, 1 H), 2.60–2.51 (m, 1 H), 2.29 (ddt, J = 14.54, 6.66, 2.58, 2.58 Hz, 1 H); ^{13}C NMR (126 MHz, $CDCl_3$) δ ppm 170.7, 135.6, 128.8, 128.1, 127.9, 47.1, 44.5, 44.2, 30.1; Data corresponded to that reported in the literature [43].

4.2.1.2. tert-Butyl 4-(3-bromo-2-oxo-pyrrolidin-1-yl)piperidine-1-carboxylate (36). Prepared according to general procedure A with *tert*-butyl 4-aminopiperidine-1-carboxylate (2.5 mmol) and 2,4-dibromobutanoyl chloride (1.2 equiv., 3 mmol); Crude product was dry loaded on silica and purified by flash column chromatography (50 g silica gel, PE/EA 1/1 1, gradient) to obtain desired product. Yield: 600 mg, 70%; Appearance: yellow oil; LCMS: 1.86 min, *m/z* 247.1, 249.1 ($(M + H)^+$ 1:1, $^{79/81}$Br), Purity>95%, Method D; ^{1}H NMR (500 MHz, $CDCl_3$) δ ppm 4.43 (dd, J = 7.16, 2.58 Hz, 1 H), 4.22 (br. s, 2 H), 4.15–4.07 (m, 1 H), 3.47 (ddd, J = 9.74, 8.02, 6.87 Hz, 1 H), 3.31 (ddd, J = 9.88, 7.88, 2.29 Hz, 1 H), 2.79 (br. s, 2 H), 2.60–2.49 (m, 1 H), 2.33 (ddt, J = 14.54, 6.52, 2.36, 2.36 Hz, 1 H), 1.79–1.71 (m, 1 H), 1.71–1.63 (m, 1 H), 1.62–1.50 (m, 2 H), 1.46 (s, 9 H); ^{13}C NMR (126 MHz, $CDCl_3$) δ ppm 170.5, 154.7, 79.9, 49.9, 44.8, 43.0, 41.2, 30.5, 29.3, 28.7, 28.5.

4.2.1.3. tert-Butyl 4-[(3-bromo-2-oxo-pyrrolidin-1-yl)methyl]piperidine-1-carboxylate (37). Prepared according to general procedure A with *tert*-butyl 4-(aminomethyl)piperidine-1-carboxylate (2.332 mmol) and 2,4-dibromobutanoyl chloride (1.2 equiv., 2.8 mmol). Crude product was dry loaded on silica and purified by flash column chromatography (50 g silica gel, PE/EA 1/9, gradient) to obtain desired product. Yield: 440 mg, 40%; Appearance: yellow oil; LCMS: 1.92 min, *m/z* 361.1, 363.1 ($(M + H)^+$ 1:1, $^{79/81}$Br), method C; ^{1}H NMR (500 MHz, $CDCl_3$) δ ppm 4.42 (dd, J = 6.87, 2.29 Hz, 1 H), 4.19–4.02 (m, 2 H), 3.66–3.59 (m, 1 H), 3.44–3.24 (m, 2 H), 3.22–3.00 (m, 1 H), 2.69 (br. s., 2 H), 2.64–2.55 (m, 1 H), 2.34 (ddt, 1 H), 1.85 (ttd, 1 H), 1.71–1.52 (m, 2 H), 1.45 (s, 9 H), 1.24–1.14 (m, 2 H); ^{13}C NMR (126 MHz, $CDCl_3$) δ ppm 171.1, 154.7, 79.4, 48.8, 46.2, 44.3, 43.4, 34.7, 30.5, 29.7, 29.5, 28.4.

4.2.1.4. 3-Bromo-1-(5-phenyl-1,3,4-oxadiazol-2-yl)pyrrolidin-2-one (38). Prepared according to general procedure A with 5-phenyl-1,3,4-oxadiazol-2-amine (1.24 mmol). and 2,4-dibromobutanoyl chloride (1.2 equiv., 1.48 mmol). Crude product was dry loaded on silica and purified by flash column chromatography (25 g silica, PE/EA 0→70%, gradient) to obtain desired product. Yield: 70 mg, 16%; Appearance: yellow oil; LCMS: 1.72 min, *m/z* 308.0, 310.0 ($(M + H)^+$ 1:1, $^{79/81}$Br), Purity = 80%, Method C; ^{1}H NMR (500 MHz, $CDCl_3$) δ ppm 8.11–8.05 (m, 2 H), 7.57–7.47 (m, 3 H), 4.60 (dd, J = 6.87, 2.86 Hz, 1 H), 4.29–4.18 (m, 2 H), 2.90–2.81 (m, 1 H), 2.60–2.53 (m, 1 H); ^{13}C NMR (126 MHz, $CDCl_3$) δ ppm 167.8, 162.5, 156.9, 131.7, 129.0, 126.7, 123.3, 45.5, 42.2, 30.3.

4.2.1.5. 3-Bromo-1-(5-phenyloxazol-2-yl)pyrrolidin-2-one (39). Prepared according to general procedure A with 5-phenyloxazol-2-amine (1.24 mmol). and 2,4-dibromobutanoyl chloride (1.2 equiv., 1.48 mmol). Crude product was dry loaded on silica and purified by flash column chromatography (25 g silica, PE/EA 0→100%) to obtain desired product. Yield: 75 mg, 18%; Appearance: yellow oil which solidified after few hours; LCMS: 1.89 min m/z 307.0, 309.0, ($(M + H)^+$ 1:1, $^{79/81}$Br), Purity = 91%, Method C; ^{1}H NMR (500 MHz, $CDCl_3$) δ ppm 7.66–7.63 (m, 2 H), 7.44–7.39 (m, 2 H), 7.32 (tt, J = 7.45, 1.70 Hz, 1 H), 7.25 (s, 1 H), 4.60 (dd, J = 6.87, 2.29 Hz, 1 H),

4.23–4.16 (m, 1 H), 4.16–4.10 (m, 1 H), 2.80 (dtd, J = 14.61, 8.16, 8.16, 6.87 Hz, 1 H), 2.54–2.47 (m, 1 H); ^{13}C NMR (126 MHz, $CDCl_3$) δ ppm 167.4, 152.0, 148.4, 128.6, 128.1, 127.1, 123.6, 120.9, 45.2, 42.9, 29.8.

4.2.1.6. 3-Bromo-1-(3,5-dimethyl-1-phenyl-pyrazol-4-yl)pyrrolidin-2-one (40). Prepared according to general procedure A with 5-phenyloxazol-2-amine (1.24 mmol). and 2,4-dibromobutanoyl chloride (1.2 equiv., 1.48 mmol). Crude product was dry loaded on silica and purified by flash column chromatography (silica gel, PE/EA 0→100% 20CV) to obtain desired product. Yield: 200 mg, 50%; Appearance: brown oil which solidified after few hours LCMS: 1.75 min m/z 334.1, 336.0 ((M + H)$^+$ 1:1, $^{79/81}$Br), Purity = 95%, Method D; ^{1}H NMR (500 MHz, $CDCl_3$) δ ppm 7.49–7.41 (m, 4 H), 7.41–7.35 (m, 1 H), 4.56 (dd, J = 6.87, 1.72 Hz, 1 H), 3.89 (ddd, J = 10.17, 8.74, 6.30 Hz, 1 H), 3.66–3.61 (m, 1 H), 2.82–2.75 (m, 1 H), 2.47 (ddt, J = 14.39, 6.23, 1.72, 1.72 Hz, 1 H), 2.25 (s, 3 H), 2.23 (s, 3 H); ^{13}C NMR (126 MHz, $CDCl_3$) δ ppm 171.0, 145.3, 139.6, 136.0, 129.2, 127.8, 124.8, 117.5, 48.6, 44.2, 31.0, 11.7, 10.8.

4.2.1.7. tert-Butyl 3-(3-bromo-2-oxo-pyrrolidin-1-yl)azetidine-1-carboxylate (41). Prepared according to general procedure A with *tert*-butyl 3-aminoazetidine-1-carboxylate (1.74 mmol) and 2,4-dibromobutanoyl chloride (1.1 equiv., 1.9 mmol). Crude product was dry loaded on silica and purified by flash column chromatography (silica gel, PE/EA 0→80%, gradient) to obtain desired product. Yield: 368 mg, 60%; Appearance: yellow oil which solidified after few hours; LCMS: 1.73 min m/z 319.1, 321.1 ((M + H)$^+$ 1:1, $^{79/81}$Br), Purity = 95%, Method D; ^{1}H NMR (500 MHz, $CDCl_3$) δ ppm 4.94 (tt, J = 8.09, 5.37 Hz, 1 H), 4.43 (dd, J = 7.16, 2.58 Hz, 1 H), 4.19 (td, J = 8.88, 4.01 Hz, 2 H), 4.01 (dd, J = 9.45, 5.44 Hz, 1 H), 3.95 (dd, J = 9.74, 5.16 Hz, 1 H), 3.71 (ddd, J = 9.74, 7.73, 6.59 Hz, 1 H), 3.58 (ddd, J = 10.02, 7.73, 2.86 Hz, 1 H) 2.68–2.59 (m, 1 H), 2.40 (ddt, J = 14.32, 6.59, 2.72, 2.72 Hz, 1 H), 1.45 (s, 9 H); ^{13}C NMR (126 MHz, $CDCl_3$) δ ppm 171.03, 156.1, 80.3, 46.2, 43.9, 41.8, 41.3, 35.2, 30.4, 28.4.

4.2.1.8. tert-Butyl (3S)-3-(3-bromo-2-oxo-pyrrolidin-1-yl)piperidine-1-carboxylate (42). Prepared according to general procedure A with *tert*-butyl (3S)-3-aminopiperidine-1-carboxylate (1.99 mmol) and 2,4-dibromobutanoyl chloride (1.2 equiv., 2.4 mmol). Crude product was dry loaded on silica and purified by flash column chromatography (silica gel, PE/EA 0 → 100%, gradient) to obtain desired product (first fraction). Yield: 300 mg, 80%; Appearance: yellow oil; LCMS: 1.87 min m/z 347.1, 349.1 ((M + H)$^+$ 1:1, $^{79/81}$Br), Purity = 90%, Method D; ^{1}H NMR (500 MHz, $CDCl_3$) δ ppm 4.41 (dd, J = 6.87, 2.29 Hz, 1 H), 3.95 (br. s., 3 H), 3.58–3.46 (m, 1 H), 3.43–3.30 (m, 1 H), 2.87 (d, J = 10.88 Hz, 1 H), 2.71 (t, J = 11.74 Hz, 1 H), 2.60–2.50 (m, 1 H), 2.38–2.26 (m, 1 H), 1.94–1.74 (m, 1 H), 1.74 (d, J = 10.31 Hz, 1 H), 1.68–1.52 (m, 2 H), 1.45 (d, J = 3.44 Hz, 9 H); ^{13}C NMR (126 MHz, $CDCl_3$) δ ppm 170.6, 154.58, 80.0, 48.9, 48.7, 44.5, 44.4, 42.2, 30.6, 28.3, 27.9, 23.9.

4.2.1.9. tert-Butyl (3S)-3-(3-bromo-2-oxo-pyrrolidin-1-yl)piperidine-1-carboxylate (43). Prepared according to general procedure A with *tert*-butyl (3S)-3-aminopiperidine-1-carboxylate (1.99 mmol) and 2,4-dibromobutanoyl chloride (1.2 equiv., 2.4 mmol). Crude product was dry loaded on silica and purified by flash column chromatography (silica gel, PE/EA 0 → 100%, gradient) to obtain desired product (second fraction). Yield: 250 mg, 80%; Appearance: yellow oil; LCMS: 1.75 min m/z 347.1, 349.1 ((M + H)$^+$ 1:1, $^{79/81}$Br), Purity = 90%, Method D; ^{1}HNMR (500 MHz, $CDCl_3$) δ ppm 4.40 (dd, J = 7.16, 2.00 Hz, 1 H), 4.07 (m, 3 H), 3.85–3.34 (dtd, J = 9.17, 5.73, 5.73, 2.86 Hz, 1 H), 3.57–3.45 (m, 1 H), 2.97–2.79 (m, 1 H), 2.69 (br t, J = 11.74 Hz, 1 H), 2.54 (dq, J = 14.75, 7.30 Hz, 1 H), 2.30 (dq, J = 14.32, 2.29 Hz, 1 H), 1.93–1.80 (m, 1 H), 1.77–1.69 (m, 1 H), 1.68–1.49 (m, 2 H), 1.45–1.42 (m, 9 H); ^{13}C NMR (126 MHz, $CDCl_3$) δ ppm 170.6, 154.5, 80.0, 48.9, 48.7, 44.4, 44.4, 42.1, 30.5, 28.3, 27.9, 23.9.

4.2.1.10. tert-Butyl 3-(3-bromo-2-oxo-pyrrolidin-1-yl)pyrrolidine-1-carboxylate (44). Prepared according to general procedure A with *tert*-butyl 3-aminopyrrolidine-1-carboxylate (1.6 mmol) and 2,4-dibromobutanoyl chloride (1.2 equiv., 1.92 mmol). Crude product was dry loaded on silica and purified by flash column chromatography (silica gel, PE/EA 0 → 100%, gradient) to obtain desired product (first fraction). Yield: 166 mg, 66%; Appearance: yellow oil; LCMS: 1.76 min m/z 332.1, 334.1 ((M + H)$^+$ 1:1, $^{79/81}$Br), Purity = 80–85%, Method D; ^{1}H NMR (500 MHz, $CDCl_3$) δ ppm 4.70 (td, J = 6.87, 13.75 Hz, 1 H), 4.41 (dd, J = 2.29, 6.87 Hz, 1 H), 4.03–4.03 (m, 1H), 3.63–3.43 (m, 4H), 3.36 (ddd, J = 2.00, 7.73, 9.74 Hz, 2 H), 2.56 (dd, J = 7.16, 14.61 Hz, 1 H), 2.34 (ddd, J = 2.86, 5.73, 11.46 Hz, 1 H), 2.22–2.07 (m, 1 H), 2.05–1.94 (m, 1 H), 1.47 (s, 9 H); ^{13}C NMR (126 MHz, $CDCl_3$) δ ppm 170.9, 154.4, 79.9, 51.6, 50.7, 48.3, 47.8, 44.4, 41.9, 30.5, 28.6, 28.1.

4.2.1.11. tert-Butyl 3-(3-bromo-2-oxo-pyrrolidin-1-yl)pyrrolidine-1-carboxylate (45). Prepared according to general procedure A with *tert*-butyl 3-aminopyrrolidine-1-carboxylate (1.6 mmol) and 2,4-dibromobutanoyl chloride (1.2 equiv., 1.92 mmol). Crude product was dry loaded on silica and purified by flash column chromatography (silica gel, PE/EA 0 → 100%, 15CV gradient) to obtain desired product (second fraction). Yield: 193 mg, 66%; Appearance: yellow oil; LCMS: 1.792 min m/z 332.1, 334.1 ((M + H)$^+$ 1:1, $^{79/81}$Br), Purity = 80–85%, Method D; ^{1}H NMR (500 MHz, $CDCl_3$) δ ppm 4.76–4.66 (m, 1 H), 4.42 (dd, J = 2.29, 6.87 Hz, 1 H), 3.65–3.44 (m, 4 H), 3.43–3.32 (m, 2 H), 2.58 (qt, J = 7.35, 14.46 Hz, 1 H), 2.39–2.31 (m, 1 H), 2.19–2.10 (m, 1 H), 2.04–1.93 (m, 1 H), 1.47 (s, 9 H); ^{13}C NMR (126 MHz, $CDCl_3$) δ ppm 171.0, 154.4, 79.9, 51.6, 47.6, 44.2, 41.9, 30.5, 28.6, 28.4.

4.2.1.12. 3-Bromo-1-(1,3-dimethylpyrazol-4-yl)pyrrolidin-2-one (46). Prepared according to general procedure A with 1,3-dimethylpyrazol-4-amine (1.8 mmol) and 2,4-dibromobutanoyl chloride (1.2 equiv., 2.16 mmol). Crude product was dry loaded on silica and purified by flash column chromatography (silica gel, PE/EA 0 → 100%, and then EA/MeOH 9/1) to obtain desired product Yield: 230 mg, 60%; Appearance: yellow oil; LCMS: 0.93 min, m/z 258.1, 260.1 ((M + H)$^+$ 1:1, $^{79/81}$Br), Purity>85%, Method D; ^{1}H NMR (500 MHz, $CDCl_3$) δ ppm 7.38 (s, 1 H), 4.52 (dd, J = 6.87, 2.29 Hz, 1 H), 3.87 (ddd, J = 10.02, 8.31, 6.30 Hz, 1 H), 3.77 (s, 3 H), 3.64 (ddd, J = 10.17, 7.88, 2.00 Hz, 1 H), 2.81–2.70 (m, 1 H), 2.45–2.38 (m, 1 H), 2.21 (s, 3 H); ^{13}C NMR (126 MHz, $CDCl_3$) δ ppm 169.9, 134.1, 133.4, 117.9, 49.0, 44.1, 36.8, 30.6, 9.8.

4.2.1.13. 3-Bromo-1-(1-isopropylpyrazol-4-yl)pyrrolidin-2-one (47). Prepared according to general procedure A with 1-isopropylpyrazol-4-amine (2.0 mmol) and 2,4-dibromobutanoyl chloride (1.2 equiv., 2.4 mmol). Crude product was dry loaded on silica and purified by flash column chromatography (silica gel, PE/EA 0 → 100%, and then EA/MeOH 9/1) to obtain desired product. Yield: 384 mg, 67%; Appearance: yellow oil; LCMS: 1.44 min, m/z 272.1, 274.1 ((M + H)$^+$ 1:1, $^{79/81}$Br), Purity>90%, Method D; ^{1}H NMR (500 MHz, DMSO-d_6) δ ppm 8.07 (s, 1 H), 7.68 (s, 1 H), 4.83 (dd, J = 7.16, 3.15 Hz, 1 H), 4.49 (quin, J = 6.59 Hz, 1 H), 3.70–3.80 (m, 2 H), 2.79 (dq, J = 14.89, 7.45 Hz, 1 H), 2.35 (ddt, J = 14.46, 6.44, 3.29, 3.29 Hz, 1 H), 1.39 (d, J = 6.87 Hz, 6 H); ^{13}C NMR (126 MHz, DMSO-d_6) δ ppm 167.3, 128.5, 122.1, 117.8, 53.3, 45.7, 43.5, 29.8, 22.6.

4.2.1.14. 3-Bromo-1-(1-phenylpyrazol-4-yl)pyrrolidin-2-one (48). Prepared according to general procedure A with 1-phenylpyrazol-4-amine (0.95 mmol) and 2,4-dibromobutanoyl chloride (1.2 equiv., 1.13 mmol). Crude product was dry loaded on silica and purified by flash column chromatography (silica gel, PE/EA 0 → 100%, and then EA/MeOH 9/1) to obtain desired product. Yield: 177 mg, 66%; Appearance: white solid; LCMS: 1.84 min, *m/z* 306.1, 308.1 ($(M + H)^+$ 1:1, $^{79/81}$Br), Purity>95%, Method D; ^{1}H NMR (500 MHz, DMSO-d_6) δ ppm 8.67 (s, 1 H), 8.08 (s, 1 H), 7.81 (d, $J = 7.45$ Hz, 2 H), 7.47 (t, $J = 8.02$ Hz, 2 H), 7.29 (t, $J = 7.34$ Hz, 1 H), 4.86 (dd, $J = 7.45$, 3.44 Hz, 1 H), 3.87–3.76 (m, 2 H), 2.82 (dq, $J = 14.46$, 7.40 Hz, 1 H), 2.41–2.34 (m, 1 H); ^{13}C NMR (126 MHz, DMSO-d_6) δ ppm 167.9, 139.5, 131.9, 129.6, 126.4, 125.3, 118.2, 117.2, 45.9, 43.7, 29.9.

4.2.1.15. 3-Bromo-1-[1-(4-pyridyl)pyrazol-4-yl]pyrrolidin-2-one (49). Prepared according to general procedure A with 1-(4-pyridyl) pyrazol-4-amine (0.65 mmol) and 2,4-dibromobutanoyl chloride (1.2 equiv., 0.8 mmol). Crude product was dry loaded on silica and purified by flash column chromatography (silica gel, PE/EA 0 → 100%, and then EA/MeOH 9/1) to obtain desired product Yield: 60 mg, 31%; Appearance: white solid; LCMS: 1.56 min, *m/z* 307.0, 309.1 ($(M + H)^+$ 1:1, $^{79/81}$Br), Purity>95%, Method D; ^{1}H NMR (500 MHz, DMSO-d_6) δ ppm 8.86 (s, 1 H), 8.61 (dd, $J = 6.30$, 1.72 Hz, 2 H), 8.21 (s, 1 H), 7.85 (dd, $J = 6.30$, 1.72 Hz, 2 H), 4.87 (dd, $J = 7.45$, 3.44 Hz, 1H), 3.88–3.77 (m, 2 H), 2.88–2.78 (m, 1 H), 2.42–2.34 (m, 1 H); ^{13}C NMR (126 MHz, DMSO-d_6) δ ppm 168.3, 149.4, 134.7, 126.0, 117.6, 112.4, 45.8, 45.6, 29.8.

4.2.1.16. 3-Bromo-1-(1-pyrimidin-2-yl-4-piperidyl)pyrrolidin-2-one (50). Prepared according to general procedure A with 1-pyrimidin-2-ylpiperidin-4-amine; dihydrochloride (0.88 mmol) and 2,4-dibromobutanoyl chloride (1.2 equiv., 1.05 mmol). Crude product was dry loaded on silica and purified by flash column chromatography (silica gel, PE/EA 0 → 100%, and then EA/MeOH 9/1) to obtain desired product Yield: 80 mg, 44%; Appearance: white solid; LCMS: 1.60 min, *m/z* 325.1, 327.1 ($(M + H)^+$ 1:1, $^{79/81}$Br), Purity>85%, Method D; ^{1}H NMR (500 MHz, DMSO-d_6) δ ppm 8.35 (d, $J = 4.58$ Hz, 2 H), 6.60 (t, $J = 5.16$ Hz, 1 H), 4.81–4.74 (m, 2 H), 4.66 (dd, $J = 10.31$, 3.44 Hz, 1 H), 4.03 (tt, $J = 11.74$, 4.30 Hz, 1 H), 3.33–3.29 (m, 2 H), 2.95–2.87 (m, 2 H), 2.58–2.57 (m, 1 H), 2.19–2.12 (m, 1 H), 1.67–1.52 (m, 4 H); ^{13}C NMR (126 MHz, DMSO-d_6) δ ppm 169.4, 161.0, 158.0, 109.9, 49.8, 46.8, 42.4, 40.9, 29.9, 27.9.

4.2.2. ***General procedure B***

3-bromopyrrolidin-2-one derivative (1 eq.) was dissolved in acetonitrile (4 mL). Under nitrogen atmosphere ammonia (32 mass %) in water (2 mL) was added to the reaction mixture. The RM was stirred overnight at 40 °C. LCMS showed only partially formed product. Acetonitrile was evaporated and remaining aq. phase was extracted with DCM. Organic phase was filtered through a phase separator and concentrated under reduced pressure to obtain desired 3-aminopyrrolidin-2-one derivative. The crude product was used in the next step without any purification step.

4.2.2.1. 3-Amino-1-benzyl-pyrrolidin-2-one (51). Product was synthesized according to general procedure B with 1-benzyl-3-bromo-pyrrolidin-2-one (**35**) (0.4 mmol). Crude product was used in the next step without any purification step. Yield: 39 mg, 60%; Appearance: yellow oil; LCMS: 1.25 min m/z 191.1, $(M + H)^+$ Purity>80%, Method D; ^{1}H NMR (500 MHz, $CDCl_3$) δ ppm 7.35–7.26 (m, 3 H), 7.24–7.20 (m, 2 H), 4.45 (d, $J = 1.72$ Hz, 2 H), 3.56 (dd, $J = 9.74$, 8.59 Hz, 1 H), 3.21–3.12 (m, 2 H), 2.43–2.35 (m, 1 H), 1.77–1.64 (m, 3 H); Compound has been reported in the literature [44].

4.2.2.2. tert-Butyl 4-(3-amino-2-oxo-pyrrolidin-1-yl)piperidine-1-carboxylate (52). Product was synthesized according to general procedure B with *tert*-butyl 4-(3-bromo-2-oxo-pyrrolidin-1-yl) piperidine-1-carboxylate (**36**) (0.79 mmol). Yield: 440 mg, 72%; Appearance: yellow oil; LCMS: 1.57 min m/z 284.0, $(M + H)^+$ Purity>90%, weak UV active, Method D; ^{1}H NMR (500 MHz, $CDCl_3$) δ ppm 4.21 (br. s., 2 H), 4.14–4.05 (m, 1 H), 3.54 (dd, $J = 9.74$, 8.59 Hz, 1 H), 3.30 (td, $J = 9.17$, 1.72 Hz, 1 H), 3.20 (td, $J = 9.45$, 6.87 Hz, 1 H), 2.79 (br. s., 2 H), 2.44 (dddd, $J = 12.67$, 8.23, 6.59, 1.72 Hz, 1 H), 1.80–1.73 (m, 2 H), 1.73–1.68 (m, 1 H), 1.68–1.53 (m, 4 H), 1.46 (s, 9 H); ^{13}C NMR (126 MHz, $CDCl_3$) δ ppm 175.3, 154.6, 79.7, 53.4, 49.3, 39.6, 29.1, 28.4.

4.2.2.3. tert-Butyl 4-[(3-amino-2-oxo-pyrrolidin-1-yl)methyl]piperidine-1-carboxylate (53). Product was synthesized according to general procedure B with *tert*-butyl 4-[(3-bromo-2-oxo-pyrrolidin-1-yl)methyl]piperidine-1-carboxylate (**37**). Yield: 128 mg, 70%; Appearance: yellow oil; LCMS: 1.67 min m/z 298.2, $(M + H)^+$ Purity>90%, weak UV active, Method D; ^{1}H NMR (500 MHz, $CDCl_3$) δ ppm 4.20–4.05 (m, 2 H), 3.58 (dd, $J = 8.59$, 9.74 Hz, 1 H), 3.35–3.29 (m, 2 H), 3.17 (br. s., 2 H), 2.73–2.63 (m, 2 H), 2.49–2.41 (m, 1 H), 2.27–2.07 (m, 2 H), 1.85–1.73 (m, 2 H), 1.64–1.54 (m, 2 H), 1.45 (s, 9 H), 1.21–1.12 (m, 2 H); ^{13}C NMR (126 MHz, $CDCl_3$) δ ppm 175.9, 154.7, 79.4, 52.9, 48.7, 44.9, 42.9, 34.6, 29.7, 28.8, 28.4.

4.2.2.4. tert-Butyl 3-(3-amino-2-oxo-pyrrolidin-1-yl)pyrrolidine-1-carboxylate (54). Product was synthesized according to general procedure B with *tert*-butyl 3-(3-bromo-2-oxo-pyrrolidin-1-yl) pyrrolidine-1-carboxylate (**44**) (0.45 mmol); Yield: 86 mg, 71%; Appearance: light orange oil; LCMS: 1.26 min, *m/z* 170.2 $(M + H)^+$, mass without BOC group Purity>90%, weak UV active, Method D; ^{1}H NMR (500 MHz, $CDCl_3$) δ ppm 4.75–4.64 (m, 1 H), 3.66–3.42 (m, 3 H), 3.41–3.18 (m, 4 H), 2.51–2.35 (m, 3 H), 2.08 (d, $J = 5.73$ Hz, 1 H), 2.03–1.89 (m, 1 H), 1.87–1.70 (m, 1 H), 1.45 (s, 9 H); ^{13}C NMR (126 MHz, $CDCl_3$) δ ppm 175.6, 154.3, 79.7, 53.4, 53.1, 50.9, 47.7, 44.7, 29.0, 28.4, 28.0.

4.2.2.5. tert-Butyl 3-(3-amino-2-oxo-pyrrolidin-1-yl)pyrrolidine-1-carboxylate (55). Product was synthesized according to general procedure B with *tert*-butyl 3-(3-bromo-2-oxo-pyrrolidin-1-yl) pyrrolidine-1-carboxylate (**45**) (0.54 mmol); Yield: 100 mg, 70%; Appearance: orange oil; LCMS: 1.47 min, *m/z* 170.2 $(M + H)^+$, mass without BOC group Purity>90%, weak UV active, Method D; ^{1}H NMR (500 MHz, $CDCl_3$) δ 4.76–4.65 (m, 1 H), 3.63–3.44 (m, 3 H), 3.42–3.18 (m, 4 H), 2.52–2.41 (m, 1 H), 2.16–2.04 (m, 1 H), 2.01–1.91 (m, 1 H), 1.88 (br. s, 2 H), 1.79–1.66 (m, 1 H), 1.46 (s, 9 H); ^{13}C NMR (126 MHz, $CDCl_3$) δ ppm 175.9, 154.3, 79.7, 53.4, 53.1, 50.3, 47.1, 44.2, 28.8, 28.4, 28.0.

4.2.2.6. tert-Butyl (3S)-3-(3-amino-2-oxo-pyrrolidin-1-yl)piperidine-1-carboxylate (56). Product was synthesized according to general procedure B with *tert*-butyl (3S)-3-(3-bromo-2-oxo-pyrrolidin-1-yl)piperidine-1-carboxylate (**42**) (0.75 mmol). Yield: 200 mg, 94%; Appearance: orange oil; LCMS: 1.60 min, *m/z* 184.2 $(M + H)^+$ mass without BOC group, Purity>80%, weak UV active, Method D; ^{1}H NMR (500 MHz, $CDCl_3$) δ ppm 4.05–3.88 (br. m, 2 H), 3.43–3.25 (br. m, 2 H), 3.16 (br. s, 2 H), 2.88–2.76 (m, 1 H), 2.66 (br. s, 1 H), 2.52–2.42 (m, 1 H), 1.84 (br. s, 2 H), 1.72 (dd, $J = 6.30$, 2.86 Hz, 1 H), 1.64–1.51 (m, 2 H), 1.44 (s, 9 H).

4.2.2.7. tert-Butyl (3S)-3-(3-amino-2-oxo-pyrrolidin-1-yl)piperidine-1-carboxylate (57). Product was synthesized according to general procedure B with *tert*-butyl (3S)-3-(3-bromo-2-oxo-pyrrolidin-1-yl)piperidine-1-carboxylate (**43**) (0.6 mmol). Yield: 107 mg, 70%; Appearance: orange oil; LCMS: 1.63 min, *m/z* 184.2

$(M + H)^+$, mass without BOC group, Purity>80%, weak UV active, Method D; ^{1}H NMR (500 MHz, $CDCl_3$) δ ppm 4.11–3.75 (m, 3 H), 3.58–3.46 (m, 1 H), 3.42–3.32 (m, 1 H), 3.31–3. 18 (m, 1 H), 2.86–2.77 (m, 1 H), 2.67 (br. s, 1 H), 2.47–2.38 (m, 1 H), 1.93 (br. s, 2 H), 1.86–1.78 (m, 1 H), 1.77–1.66 (m, 2 H), 1.65–1.50 (m, 2 H), 1.43 (s, 9 H).

4.2.2.8. tert-Butyl 3-(3-amino-2-oxo-pyrrolidin-1-yl)azetidine-1-carboxylate (58). Product was synthesized according to general procedure B with *tert*-butyl 3-(3-bromo-2-oxo-pyrrolidin-1-yl) azetidine-1-carboxylate (**41**) (1.1 mmol). Yield: 220 mg, 79%; Appearance: yellow oil; LCMS: 1.37 min, *m/z* 156.2 $(M + H)^+$ mass without BOC group, Purity>90%, weak UV active, Method D; ^{1}H NMR (500 MHz, $CDCl_3$) δ ppm 4.99–4.91 (m, 1 H), 4.19–4.09 (m, 2 H), 3.97 (dd, $J = 6.87, 5.73$ Hz, 2 H), 3.56 (dd, $J = 9.74, 8.02$ Hz, 2 H), 3.42 (td, $J = 9.74, 6.87$ Hz, 1 H), 2.51 (dddd, $J = 12.67, 8.09, 6.73, 1.72$ Hz, 1 H), 1.84 (br. s, 2 H), 1.81–1.72 (m, 1 H), 1.44 (s, 9 H); ^{13}C NMR (126 MHz, $CDCl_3$) δ ppm 176.0, 156.0, 80.0, 53.2, 52.6, 41.1, 39.7, 28.6, 28.2.

4.2.2.9. 3-Amino-1-(5-phenyl-1,3,4-oxadiazol-2-yl)pyrrolidin-2-one (59). Product was synthesized according to general procedure B with 3-bromo-1-(5-phenyl-1,3,4-oxadiazol-2-yl)pyrrolidin-2-one (**38**). Yield: 12 mg, 20%; Appearance: white solid; LCMS: 1.336 min, *m/z* 245 $(M + H)^+$ Purity>80%, Method D; ^{1}H NMR (500 MHz, CD_3OD) δ ppm 7.91–7.85 (m, 2 H), 7.58–7.49 (m, 3 H), 4.69 (d, $J = 4.58$ Hz, 1 H), 3.58–3.50 (m, 1 H), 3.42–3.34 (m, 1 H), 2.25–2.19 (m, 1 H), 2.10–2.01 (m, 1 H).

4.2.2.10. 3-Amino-1-(3,5-dimethyl-1-phenyl-pyrazol-4-yl)pyrrolidin-2-one (60). Product was synthesized according to general procedure B with 3-bromo-1-(3,5-dimethyl-1-phenyl-pyrazol-4-yl)pyrrolidin-2-one (**40**) (0.39 mmol). Yield: 40 mg, 38%; Appearance: yellowish oil; LCMS: 1.39 min m/*z* 271.2, $(M + H)^+$ Purity>90%, Method D; ^{1}H NMR (500 MHz, $CDCl_3$) δ ppm 7.50–7.41 (m, 4 H), 7.40–7.34 (m, 1 H), 3.74 (dd, $J = 10.31, 8.02$ Hz, 1 H), 3.65 (td, $J = 9.74, 6.87$ Hz, 1 H), 3.56 (td, $J = 9.45, 1.72$ Hz, 1 H), 2.63–2.55 (m, 1 H), 2.23–2.22 (s, 3 H), 2.21–2.19 (s, 3 H), 1.97 (dq, $J = 12.60, 9.36$ Hz, 1 H), 1.82–1.65 (m, 2 H); ^{13}C NMR (126 MHz, $CDCl_3$) δ ppm 176.0, 145.0, 139.5, 135.5, 129.1, 127.6, 124.6, 118.3, 52.8, 47.1, 29.6, 11.7, 10.9.

4.2.2.11. 3-Amino-1-(1,3-dimethylpyrazol-4-yl)pyrrolidin-2-one (61). Product was synthesized according to general procedure B with 3-bromo-1-(1,3-dimethylpyrazol-4-yl)pyrrolidin-2-one (**36**), (0.73 mmol). Yield: 150 mg, 84%; Appearance: yellowish oil; LCMS: 0.29 min m/*z* 195.2, $(M + H)^+$ Purity>90%, Method C; ^{1}H NMR (500 MHz, DMSO-d_6) δ 7.34–7.32 (m, 1H), 3.71–3.68 (s, 3H), 3.57–3.51 (m, 1H), 3.48–3.46 (m, 1H), 3.46–3.43 (m, 1H), 2.31 (dddd, $J = 2.00, 6.59, 8.31, 12.32$ Hz, 1H), 2.11 (s, 3H), 1.82–1.69 (m, 1H); ^{13}C NMR (126 MHz, DMSO-d_6) δ ppm 175.2, 133.2, 133.0, 119.2, 52.4, 46.9, 36.5, 28.9, 9.5; The NMR analysis showed rotamers.

4.2.2.12. 3-Amino-1-(1-isopropylpyrazol-4-yl)pyrrolidin-2-one (62). Product was synthesized according to general procedure B with 3-bromo-1-(1-isopropylpyrazol-4-yl)pyrrolidin-2-one (**47**) (0.57 mmol). Yield: 125 mg, 94%; Appearance: off-white solid; LCMS: 0.98 min, *m/z* 209.2 $(M + H)^+$ Purity>90%, Method D; ^{1}H NMR (500 MHz, DMSO-d_6) δ ppm 7.97 (s, 1 H), 7.61 (s, 1 H), 4.45 (quin, $J = 6.73$ Hz, 1 H), 3.65–3.57 (m, 2 H), 3.56–3.48 (m, 1 H), 2.41–2.33 (m, 1 H), 1.85–1.75 (m, 1 H), 1.35 (d, $J = 6.30$ Hz, 6 H); ^{13}C NMR (126 MHz, DMSO-d_6) δ ppm 171.8, 128.3, 122.5, 117.2, 53.2, 52.1, 44.2, 27.3, 22.6.

4.2.2.13. 3-Amino-1-(1-phenylpyrazol-4-yl)pyrrolidin-2-one (63). Product was synthesized according to general procedure B with 3-bromo-1-(1-phenylpyrazol-4-yl)pyrrolidin-2-one (**48**) (0.2 mmol). Yield: 50 mg, 95%; Appearance: orange oil; LCMS: 1.46 min, *m/z* 243.2 $(M + H)^+$ Purity>95%, Method D; ^{1}H NMR (500 MHz, DMSO-d_6) δ ppm 8.61 (s, 1 H), 8.09 (s, 1 H), 7.86–7.80 (m, 2 H), 7.54–7.47 (m, 2 H), 7.34–7.27 (m, 1 H), 3.70 (td, $J = 9.45, 2.29$ Hz, 1 H), 3.65–3.53 (m, 1 H), 2.45–2.38 (m, 1 H), 1.81 (dq, $J = 12.32, 9.26$ Hz, 1 H); ^{13}C NMR (126 MHz, DMSO-d_6) δ ppm 174.8, 140.1, 132.4, 130.2, 126.8, 126.0, 118.5, 116.9, 53.4, 44.7, 29.0.

4.2.2.14. 3-Amino-1-[1-(4-pyridyl)pyrazol-4-yl]pyrrolidin-2-one (64). Product was synthesized according to general procedure B with 3-bromo-1-[1-(4-pyridyl)pyrazol-4-yl]pyrrolidin-2-one (**49**) (0.16 mmol). Yield: 50 mg, 95%; Appearance: orange oil; LCMS: 1.46 min, *m/z* 243.2 $(M + H)^+$ Purity>95%, Method D; ^{1}H NMR (500 MHz, DMSO-d_6) δ ppm 8.90 (s, 1 H), 8.67–8.63 (m, 2 H), 8.28 (s, 1 H), 7.94–7.84 (m, 2 H), 4.25 (t, $J = 9.45$ Hz, 1 H), 3.91–3.82 (m, 1 H), 3.81–3.72 (m, 1 H), 2.64–2.55 (m, 1 H), 2.21–2.08 (m, 1 H); ^{13}C NMR (126 MHz, DMSO-d_6) δ ppm 167.8, 151.3, 145.2, 133.8, 125.3, 117.3, 111.9, 50.2, 44.8, 24.0.

4.2.2.15. 3-Amino-1-(1-pyrimidin-2-yl-4-piperidyl)pyrrolidin-2-one (65). Product was synthesized according to general procedure B with 3-bromo-1-(1-pyrimidin-2-yl-4-piperidyl)pyrrolidin-2-one (**50**) (0.2 mmol). Yield: 60 mg, 90% Appearance: off-white solid; LCMS: 1.18 min, *m/z* 262.2 $(M + H)^+$ Purity>90%, Method D; ^{1}H NMR (500 MHz, DMSO-d_6) δ ppm 8.31 (d, $J = 4.58$ Hz, 2 H), 6.56 (t, $J = 4.58$ Hz, 1 H), 4.77–4.70 (m, 2 H), 4.03–3.93 (m, 1 H), 3.27 (dd, $J = 9.74, 8.02$ Hz, 1 H), 3.18 (td, $J = 9.17, 2.29$ Hz, 1 H), 3.05 (td, $J = 9.45, 6.87$ Hz, 1 H), 2.92–2.81 (m, 2 H), 2.16 (dddd, $J = 12.17, 8.16, 6.59, 1.72$ Hz, 1 H), 1.79 (br s, 1 H), 1.61–1.43 (m, 4 H); ^{13}C NMR (126 MHz, DMSO-d_6) δ ppm 175.0, 161.0, 158.0, 1099, 53.0, 49.2, 42.5, 42.5, 28.6, 28.5.

4.2.3. General procedure C

To a solution of amine (1 equiv.) in dichloromethane at room temperature was added the appropriate isocyanate (1.1 equiv.) and triethylamine (1.5 equiv.). The resulting mixture was stirred at room temperature for 3 h. RM was concentrated and purified by either flash column chromatography or by preparative HPLC (19 × 100mm (5 μm) C-18 Waters Xbridge, MeOH pH = 10) to yield final urea product as a white solid.

4.2.3.1. 1-(1-Benzyl-2-oxo-pyrrolidin-3-yl)-3-(4-bromophenyl)urea (9). Prepared according to modified procedure C with intermediate 3-amino-1-benzyl-pyrrolidin-2-one (**51**) (0.18 mmol) and 4-bromophenyl isocyanate (1.1 equiv., 0.20 mmol). Crude product was purified by reverse phase column chromatography (C18, acetonitrile/water pH = 10). Yield: 42 mg, 62%; Appearance: white solid; LCMS: 2.06 min m/*z* 388.1, 390.1 ($(M + H)^+$ 1:1, $^{79/81}$Br), Method D; ^{1}H NMR (500 MHz, DMSO-d_6) δ ppm 8.81 (s, 1 H), 7.42–7.33 (m, 6 H), 7.31–7.21 (m, 4 H), 6.60 (d, $J = 6.87$ Hz, 1 H), 4.47–4.36 (m, 2 H), 4.36–4.27 (m, 1 H), 3.26–3.14 (m, 2 H), 2.41–2.33 (m, 1 H), 1.88–1.78 (m, 1 H); ^{13}C NMR (126 MHz, DMSO-d_6) δ ppm 172.3, 154.8, 139.7, 136.6, 131.4, 128.6, 127.6, 119.6, 119.5, 112.5, 51.1, 46.1, 43.0, 26.9; HRMS: Exact Mass: 387.0582; $(M + H)^+$: 388.0662; Observed mass: 388.0668; 1.45 ppm.

4.2.3.2. tert-Butyl 4-[3-[(4-bromophenyl) carbamoylamino] -2-oxo-pyrrolidin-1-yl] piperidine-1-carboxylate (10). Prepared according to modified procedure C with intermediate *tert*-butyl 4-(3-amino-2-oxo-pyrrolidin-1-yl)piperidine-1-carboxylate (**52**) (0.25 mmol) and 4-bromophenyl isocyanate (1.1 equiv., 0.27 mmol); Crude compound was dry loaded on silica and purified by flash column

chromatography (silica gel, PE/EtOAc 0–100%). Yield: 65 mg, 49%; Appearance: white solid; LCMS: 2.15 min m/*z* 481.1, 483.1 ((M + H)$^+$ 1:1, $^{79/81}$Br), Purity = 90%, Method D; ^{1}H NMR (500 MHz, $CDCl_3$) δ ppm 7.96 (br. s, 1 H), 7.28–7.26 (m, 2 H), 7.14 (d, J = 8.59 Hz, 2 H), 6.33 (br. s, 1 H), 4.39–4.27 (m, 1 H), 4.27–4.13 (m, 2 H), 4.12–4.04 (m, 1 H), 3.46–3.38 (m, 1 H), 3.34–3.27 (m, 1 H), 2.74 (br. s, 2 H), 2.68–2.60 (m, 1 H), 2.07–1.96 (m, 1 H), 1.69–1.56 (m, 4 H), 1.47 (s, 9 H); ^{13}C NMR (126 MHz, $CDCl_3$) δ ppm 173.6, 155.6, 154.5, 138.2, 131.5, 120.6, 114.8, 80.0, 53.07, 50.1, 42.9, 40.5, 29.1, 28.7, 28.4; HRMS: Exact mass: 480.1372; (M + H)$^+$:481.1452; Observed mass: 481.1446; 1.29 ppm.

4.2.3.3. tert-Butyl 4-[[3-[(4-bromophenyl)carbamoylamino]-2-oxo-pyrrolidin-1-yl]methyl] piperidine-1-carboxylate (11). Prepared according to modified procedure C with intermediate *tert*-butyl 4-[(3-amino-2-oxo-pyrrolidin-1-yl)methyl]piperidine-1-carboxylate (**53**) (0.37 mmol) and 4-bromophenyl isocyanate (1.1 equiv., 0.41 mmol); Crude compound was dry loaded on silica and purified by flash column chromatography (silica gel, DCM/MeOH 97/3). Yield: 160 mg, 83%; Appearance: white solid; LCMS: 2.20 min m/*z* 495.1, 497.1 ((M + H)$^+$ 1:1, $^{79/81}$Br), Purity = 95%, Method D; ^{1}H NMR (500 MHz, $CDCl_3$) δ ppm 7.93 (br. s, 1 H), 7.23 (d, J = 8.59 Hz, 2 H), 7.10 (d, J = 8.59 Hz, 2 H), 6.50 (br. s., 1 H), 4.39–4.23 (m, 1 H), 4.13 (d, J = 6.87 Hz, 2 H), 3.51–3.39 (m, 2 H), 3.32–3.13 (m, 2 H), 2.69 (br. s., 2 H), 2.61 (br. s, 1 H), 2.22–2.05 (m, 1 H), 1.81 (dtt, J = 11.17, 7.45, 7.45, 3.87, 3.87 Hz, 1 H), 1.68–1.56 (m, 2 H), 1.45 (s, 9 H), 1.20–1.08 (m, 2 H); ^{13}C NMR (126 MHz, $CDCl_3$) δ ppm 174.6, 155.7, 154.8, 138.3, 131.6, 120.8, 114.9, 79.7, 52.7, 49.2, 45.6, 43.2, 34.5, 29.8, 28.6, 28.5; HRMS: Exact Mass: 494.1529; (M + H)$^+$: 495.1609; Observed mass: 495.1599; 2.02 ppm.

4.2.3.4. tert-Butyl 3-[3-[(4-bromophenyl)carbamoylamino]-2-oxo-pyrrolidin-1-yl]azetidine-1-carboxylate (14). Prepared according to modified procedure A with intermediate *tert*-butyl 3-(3-amino-2-oxo-pyrrolidin-1-yl)azetidine-1-carboxylate (**58**) (0.29 mmol) and 4-bromophenyl isocyanate (1.1 equiv., 0.32 mmol); Crude compound was dry loaded on silica and purified by flash column chromatography (silica gel, DCM/MeOH 97/3). Yield: 62 mg, 44%; Appearance: beige solid; LCMS: 2.090 min m/*z* 453, 455 ((M + H)$^+$ 1:1, $^{79/81}$Br), Purity = 95%, Method D; ^{1}H NMR (500 MHz, $CDCl_3$) δ ppm 7.79 (br. s., 1 H), 7.28–7.27 (m, 1 H), 7.27–7.25 (m, 1 H), 7.13–7.09 (m, 2 H), 6.27 (d, J = 5.73 Hz, 1 H), 4.89 (tt, J = 8.16, 5.59 Hz, 1 H), 4.31 (dd, J = 7.45, 5.16 Hz, 1 H), 4.17 (td, J = 8.88, 5.16 Hz, 2 H), 4.03 (dt, J = 9.88, 5.08 Hz, 2 H), 3.67 (td, J = 8.02, 2.86 Hz, 1 H), 3.51 (td, J = 9.59, 7.16 Hz, 1 H), 2.72–2.63 (m, 1 H), 2.16–2.05 (m, 1 H), 1.45 (s, 9 H); ^{13}C NMR (126 MHz, $CDCl_3$) δ ppm 174.3, 156.0, 155.5, 137.9, 131.6, 120.8, 115.1, 80.3, 52.9, 52.4, 41.8, 40.8, 28.3, 27.2; HRMS: Exact mass: 452.1059; 453.1139; (M + H)$^+$ Observed mass: 453.1127; 2.65 ppm.

4.2.3.5. tert-Butyl (3S)-3-[3-[(4-bromophenyl)carbamoylamino]-2-oxo-pyrrolidin-1-yl] piperidine-1-carboxylate (19). Prepared according to modified procedure C with intermediate *tert*-butyl (3S)-3-(3-amino-2-oxo-pyrrolidin-1-yl)piperidine-1-carboxylate (**56**) (0.6 mmol) and 4-bromophenyl isocyanate (1.1 equiv., 0.66 mmol); Crude compound was dry loaded on silica and purified by flash column chromatography (silica gel, DCM/MeOH 97/3). Yield: 150 mg, 49% Appearance: beige solid; LCMS: 2.129 min m/*z* 481, 483 ((M + H)$^+$ 1:1, $^{79/81}$Br), Purity = 85%, Method D; ^{1}H NMR (500 MHz, DMSO-d_6) δ ppm 8.83–8.72 (m, 1 H), 7.41–7.34 (m, 4 H), 6.56–6.48 (m, 1 H), 4.30–4.22 (m, 1 H), 3.83 (d, J = 9.74 Hz, 2 H), 3.76–3.65 (m, 1 H), 3.39–3.34 (m, 1 H), 3.33–3.30 (m, 1 H), 3.30–3.19 (m, 1 H), 2.95–2.74 (m, 1 H), 2.41–2.32 (m, 1 H), 1.80–1.65 (m, 3 H), 1.59 (qd, J = 12.03, 3.44 Hz, 1 H), 1.41–1.38 (m, 9 H), 1.37 (br. s, 1 H); ^{13}C NMR (126 MHz, DMSO-d_6) δ ppm 172.0, 154.8, 153.9, 139.7, 131.4, 119.6, 112.5, 78.9, 54.9, 51.3, 48.6, 48.2, 28.1, 27.4, 27.3, 24.0; HRMS: Exact Mass: 480.1372; (M + H)$^+$ 481.1452; Observed mass: 481.1443; 1.87 ppm.

4.2.3.6. tert-Butyl (3S)-3-[3-[(4-bromophenyl)carbamoylamino]-2-oxo-pyrrolidin-1-yl] piperidine-1-carboxylate (20). Prepared according to modified procedure C with intermediate *tert*-butyl (3S)-3-(3-amino-2-oxo-pyrrolidin-1-yl)piperidine-1-carboxylate (**57**) (0.3 mmol) and 4-bromophenyl isocyanate (1.1 equiv., 0.33 mmol); Crude compound was dry loaded on silica and purified by flash column chromatography (silica gel, DCM/MeOH 97/3). Yield: 125 mg, 54%; Appearance: beige solid; LCMS: 2.13 min m/*z* 481.1, 483.1 ((M + H)$^+$ 1:1, $^{79/81}$Br), Purity = 85%, Method D; ^{1}H NMR (500 MHz, DMSO-d_6) δ ppm 8.78 (s, 1 H), 7.41–7.35 (m, 4 H), 6.55–6.49 (m, 1 H), 4.32–4.22 (m, 1 H), 3.83 (br.d, 2 H) 3.74–3.65 (m, 1 H) 3.39–3.34 (m, 1 H) 3.30–3.19 (m, 1 H) 2.96–2.59 (m, 2 H) 2.41–2.32 (m, 1 H) 1.81–1.64 (m, 4 H) 1.64–1.51 (m, 1 H) 1.40 (d, J = 2.29 Hz, 9 H); ^{13}C NMR (126 MHz, DMSO-d_6) δ ppm 172.0, 154.8, 153.8, 139.7, 131.4, 119.6, 112.5, 78.9, 51.4, 51.3, 48.2, 28.1, 27.4, 27.3, 27.0; 1 carbon hidden under DMSO peak; HRMS: Exact Mass: 480.1372; (M + H)$^+$ 481.1452; Observed mass:481.145; 0.42 ppm.

4.2.3.7. tert-Butyl 3-[3-[(4-bromophenyl)carbamoylamino]-2-oxo-pyrrolidin-1-yl] pyrrolidine-1-carboxylate (66). Prepared according to modified procedure C with intermediate *tert*-butyl 3-(3-amino-2-oxo-pyrrolidin-1-yl)pyrrolidine-1-carboxylate (**54**) (0.3 mmol) and 4-bromophenyl isocyanate (1.1 equiv., 0.33 mmol); Crude compound was dry loaded on silica and purified by flash column chromatography (silica gel, DCM/MeOH 97/3). Yield: 90 mg, 60%; Appearance: beige solid; LCMS: 2.12 min m/*z* 467.1, 469.1 ((M + H)$^+$ 1:1, $^{79/81}$Br), Purity = 85%, Method D; ^{1}H NMR (500 MHz, $CDCl_3$) δ ppm 7.98 (br. s., 1 H), 7.25 (br. s, 2 H), 7.13 (br. s., 2 H), 6.51–6.32 (m, 1 H), 4.72–4.63 (m, 1 H), 4.32–4.21 (m, 1 H), 3.61–3.51 (m, 2 H), 3.50–3.43 (m, 2 H), 3.43–3.28 (m, 3 H), 2.68–2.58 (m, 1 H), 2.11 (br. s, 1 H), 2.08–1.93 (m, 2 H), 1.47 (s, 9 H), *broad peaks, possible rotamers*; ^{13}C NMR (126 MHz, $CDCl_3$) δ ppm 174.2, 155.6, 154.3, 138.1, 131.6, 120.6, 114.9, 80.0, 52.9, 51.6, 51.1, 47.7, 44.6, 29.1, 28.4, 27.9.

4.2.3.8. ***tert-Butyl 3-[3-[(4-bromophenyl)carbamoylamino]-2-oxo-pyrrolidin-1-yl] pyrrolidine-1-carboxylate*** *(**67**).* Prepared according to modified procedure C with intermediate *tert*-butyl 3-(3-amino-2-oxo-pyrrolidin-1-yl)pyrrolidine-1-carboxylate (**55**) (0.24 mmol) and 4-bromophenyl isocyanate (1.1 equiv., 0.27 mmol); Crude compound was dry loaded on silica and purified by flash column chromatography (silica gel, DCM/MeOH 97/3). Yield: 50 mg, 44%; Appearance: beige solid; LCMS: 2.13 min m/*z* 467.1, 469.1 ((M + H)$^+$ 1:1, $^{79/81}$Br), Purity = 85%, Method D; ^{1}H NMR (500 MHz, CD_3OD) δ ppm 7.37–7.27 (m, 4 H), 4.65–4.55 (m, 1 H), 4.43–4.30 (m, 1 H), 3.60–3.46 (m, 2 H), 3.45–3.40 (m, 1 H), 3.40–3.31 (m, 3 H), 2.54–2.44 (m, 1 H), 2.16–1.85 (m, 3 H), 1.45 (s, 9 H), *broad peaks*, *possible rotamer*; ^{13}C NMR (126 MHz, CD_3OD) δ ppm 173.9, 156.1, 154.9, 138.8, 131.4, 120.4, 114.3, 79.9, 52.1, 51. 8, 44.5, 44.0, 40.5, 28.3, 27.4, 26.7.

4.2.3.9. 1-(4-Bromophenyl)-3-[1-(3,5-dimethyl-1-phenyl-pyrazol-4-yl)-2-oxo-pyrrolidin-3-yl]urea (21). Prepared according to modified procedure C with intermediate 3-amino-1-(3,5-dimethyl-1-phenyl-pyrazol-4-yl)pyrrolidin-2-one (**60**) (0.11 mmol) and 4-bromophenyl isocyanate (1.1 equiv., 0.12 mmol); Crude compound was purified by reverse phase column chromatography (MeOH/water pH = 10). Yield: 47 mg, 90%; Appearance: white solid; LCMS: 2.094 min m/*z* 468, 470 ((M + H)$^+$ 1:1, $^{79/81}$Br), Purity = 95%, Method D; ^{1}H NMR (500 MHz, DMSO-d_6) δ ppm 8.81 (s, 1 H), 7.48 (d, J = 4.58 Hz, 4 H), 7.42–7.34 (m, 5 H), 6.63 (d,

J = 6.87 Hz, 1 H), 4.46 (ddd, J = 10.45, 8.74, 7.16 Hz, 1 H), 3.68–3.61 (m, 1 H), 3.47 (dt, J = 8.59, 1.72 Hz, 1 H), 2.17 (s, 3 H), 2.09–2.01 (m, 2 H); ^{13}C NMR (126 MHz, DMSO-d_6) δ ppm 173.0, 155.3, 145.3, 140.2, 140.0, 136.0, 131.9, 129.8, 127.8, 124.4, 120.2, 119.5, 113.1, 51.3, 47.1, 28.1, 11.9, 11.1; HRMS: Exact Mass: 467.0957; $(M + H)^+$ 468.1037; Observed mass: 468.103; 1.5 ppm.

4.2.3.10. 1-(4-Bromophenyl)-3-[2-oxo-1-(1-pyrimidin-2-yl-4-piperidyl)pyrrolidin-3-yl]urea (22). Prepared according to modified procedure C with intermediate 3-amino-1-(1-pyrimidin-2-yl-4-piperidyl)pyrrolidin-2-one (**65**) (0.14 mmol) and 4-bromophenyl isocyanate (1.1 equiv., 0.155 mmol); Crude compound was purified by preparative HPLC (19 × 100mm (5 μm) C-18 Waters Xbridge, MeOH pH = 10); Yield: 38 mg, 60%; Appearance: white solid; LCMS: 1.99 min, *m/z* 459.0, 461.0 ($(M + H)^+$ 1:1, $^{79/81}$Br), Purity = 95%, Method D; ^{1}H NMR (500 MHz, DMSO-d_6) δ 8.80 (s, 1H), 8.35 (d, J = 4.58 Hz), 7.35–7.41 (m, 4H), 6.60 (t, J = 4.58 Hz, 1 H), 6.53 (d, J = 6.87 Hz, 1 H), 4.74–4.82 (m, 2 H), 4.25 (ddd, J = 6.87, 8.59, 10.31 Hz, 1 H), 4.02–4.11 (m, 1 H), 3.26–3.32 (m, 1 H), 3.15–3.22 (m, 1 H), 2.86–2.97 (m, 2 H), 2.32–2.40 (m, 1 H), 1.69–1.77 (m, 1 H), 1.48–1.69 (m, 4 H); ^{13}C NMR (126 MHz, DMSO-d_6) δ ppm 171.6, 161.0, 158.2, 154.8, 139.7, 131.4, 119.3, 112.5, 109.9, 51.6, 49.5, 42.5, 28.3, 27.3; HRMS: Exact Mass: 458.1066; $(M + H)^+$:459.1146; Observed Mass: 459.1142; 0.87 ppm.

4.2.3.11. 1-(4-Bromophenyl)-3-[1-(1,3-dimethylpyrazol-4-yl)-2-oxo-pyrrolidin-3-yl]urea (30). Prepared according to modified procedure C with intermediate 3-amino-1-(1,3-dimethylpyrazol-4-yl) pyrrolidin-2-one (**61**) (0.26 mmol) and 4-bromophenyl isocyanate (1.1 equiv., 0.28 mmol); Crude compound was purified by reverse phase column chromatography (MeOH/water pH = 10); Yield: 35 mg, 35%; Appearance: white solid; LCMS: 1.78 min m/*z* 392.1, 394.1 ($(M + H)^+$ 1:1, $^{79/81}$Br), Purity>95%, Method D; ^{1}H NMR (500 MHz, DMSO-d_6) δ ppm 8.92 (s, 1 H), 7.39 (s, 4 H), 7.36 (s, 1 H), 6.73 (d, J = 6.87 Hz, 1 H), 4.41 (ddd, J = 10.45, 8.74, 7.16 Hz, 1 H), 3.71 (s, 3 H), 3.65 (td, J = 9.59, 6.59 Hz, 1 H), 3.45–3.55 (m, 1 H), 2.41–2.48 (m, 1 H), 2.14 (s, 3 H), 2.00 (dd, J = 12.60, 10.31 Hz, 1 H); ^{13}C NMR (126 MHz, DMSO-d_6) δ ppm 171.6, 154.8, 139.8, 133.5, 133.1, 131.4, 119.7, 119.0, 112.5, 50.9, 46.9, 36.6, 27.3, 9.4; HRMS: Exact Mass: 391.0644; $(M + H)^+$:392.0724; Observed Mass: 392.0719; 1.28 ppm.

4.2.3.12. 1-(4-Bromophenyl)-3-[1-(1-isopropylpyrazol-4-yl)-2-oxo-pyrrolidin-3-yl]urea (31). Prepared according to modified procedure C with intermediate 3-amino-1-(1-isopropylpyrazol-4-yl)pyrrolidin-2-one (**62**) (0.24 mmol) and 4-bromophenyl isocyanate (1.1 equiv., 0.264 mmol); Crude compound was purified by preparative HPLC (19 × 100mm (5 μm) C-18 Waters Xbridge, MeOH pH = 10); Yield: 38 mg, 39%; Appearance: white solid; LCMS: 1.92 min m/*z* 406.1, 408.0 ($(M + H)^+$ 1:1, $^{79/81}$Br), Purity>95%, Method D; ^{1}H NMR (500 MHz, DMSO-d_6) δ ppm 8.87 (s, 1 H), 8.01 (s, 1 H), 7.66 (s, 1 H), 7.45–7.33 (m, 4 H), 6.63 (d, J = 7.45 Hz, 1 H), 4.49 (quin, J = 6.59 Hz, 1 H), 4.42 (ddd, J = 10.17, 8.74, 7.45 Hz, 1 H), 3.71–3.64 (m, 1 H), 3.63–3.55 (m, 1 H), 2.49–2.46 (m, 1 H), 2.01 (dd, J = 12.32, 10.02 Hz, 1 H), 1.39 (d, J = 6.30 Hz, 6 H); ^{13}C NMR (126 MHz, DMSO-d_6) δ ppm 170.5, 155.3, 140.2, 131.9, 128.8, 123.2, 120.2, 117.7, 113.1, 53.7, 51.8, 44.6, 27.3, 23.2; HRMS: Exact Mass: 405.0800; $(M + H)^+$: 406.088; Observed Mass: 406.0872; 1.97 ppm.

4.2.3.13. 1-(4-Bromophenyl)-3-[2-oxo-1-[1-(4-pyridyl)pyrazol-4-yl] pyrrolidin-3-yl]urea (32). Prepared according to modified procedure A with intermediate 3-amino-1-[1-(4-pyridyl)pyrazol-4-yl] pyrrolidin-2-one (**64**) (0.24 mmol) and 4-bromophenyl isocyanate (1.1 equiv., 0.264 mmol); Crude compound was purified by preparative HPLC (19 × 100mm (5 μm) C-18 Waters Xbridge, MeOH pH = 1). the compound was dissolved in MeOH and passed through the Isolute SPE column (500 mg) to obtain desired product as free base.; Yield: 28 mg, 51%; Appearance: white solid; LCMS: 1.92 min, *m/z* 441.0, 443.0 ($(M + H)^+$ 1:1, $^{79/81}$Br), Purity>95%, Method D; ^{1}H NMR (500 MHz, DMSO-d_6) δ ppm 8.88 (s, 1 H, NH) 8.77 (s, 1 H) 8.63–8.59 (m, 2 H) 8.22 (s, 1 H) 7.86–7.81 (m, 2 H) 7.40–7.34 (m, 4 H) 6.66 (d, J = 7.45 Hz, 1 H) 4.51–4.43 (m, 1 H) 3.79–3.62 (m, 2 H), 2.53–2.49 (m, 1 H) 2.13–2.02 (m, 1 H); ^{13}C NMR (126 MHz, DMSO-d_6) δ ppm 171.5, 155.2, 151.7, 145.8, 140.2, 134.2, 131.9, 126.8, 120.3, 117.0, 113.1, 112.3, 51.8, 44.7, 27.0; HRMS: Exact Mass: 440.0596; $(M + H)^+$: 441.0676; Observed Mass: 441.0669; 1.59 ppm.

4.2.3.14. 1-(4-Bromophenyl)-3-[2-oxo-1-(1-phenylpyrazol-4-yl)pyrrolidin-3-yl]urea (33). Prepared according to modified procedure C with intermediate 3-amino-1-(1-phenylpyrazol-4-yl)pyrrolidin-2-one (**63**) (0.16 mmol) and 4-bromophenyl isocyanate (1.1 equiv., 0.18 mmol); Crude compound was purified by preparative HPLC (19 × 100mm (5 μm) C-18 Waters Xbridge, MeOH pH = 10).; Yield: 12 mg, 16%; Appearance: white solid; LCMS: 2.09 min, *m/z* 440.0, 442.0 ($(M + H)^+$ 1:1, $^{79/81}$Br), Purity>95%, Method D; ^{1}H NMR (500 MHz, DMSO-d_6) δ 8.88 (s, 1 H), 8.60 (s, 1 H), 8.08 (s, 1 H), 7.80 (d, J = 8.02 Hz, 2 H), 7.47 (dd, J = 7.45, 8.59 Hz, 2 H), 7.39–7.33 (m, 4 H), 7.28 (t, J = 7.39 Hz, 1 H), 6.65 (d, J = 7.45 Hz, 1 H), 4.46 (ddd, J = 7.45, 8.88, 10.02 Hz, 1 H), 3.77–3.70 (m, 1 H), 3.69–3.63 (m, 1 H), 2.53–2.49 (m, 1 H), 2.10–2.00 (m, 1 H); ^{13}C NMR (126 MHz, DMSO-d_6) δ ppm 170.7, 154.7, 139.7, 139.5, 131.7, 131.4, 129.6, 126.2, 125.4, 119.7, 118.0, 116.4, 112.6, 51.2, 44.2, 26.6; HRMS: Exact Mass: 439.0644; $(M + H)^+$:440.0724; Observed Mass: 440.0715; 2.05 ppm.

4.2.4. Compound were synthesized according to general procedure D: BOC deprotection

Starting material was dissolved in dichloromethane and hydrochloric acid (4 mol/l) in 1,4-dioxane (5–10 equiv.) was added. Reaction mixture was stirred at room temperature for 2.5 h. A crude product was dissolved in methanol. Methanol solution was passed through the Isolute NH_2 SPE cartridge and filtrate was concentrated under reduced pressure to get desired product as a free base.

4.2.4.1. 1-(4-Bromophenyl)-3-[2-oxo-1-(4-piperidyl)pyrrolidin-3-yl] urea (13). Compound was prepared according to general procedure D with intermediate: *tert*-butyl 4-[3-[(4-bromophenyl) carbamoylamino] -2-oxo-pyrrolidin-1-yl] piperidine-1-carboxylate (**10**) (0.11 mmol). A crude product was dissolved in methanol. Methanol solution was passed through the Isolute NH_2 SPE cartridge (500 mg) and filtrate was concentrated under reduced pressure to give the desired product as a free base. Yield: 40 mg, 92%; Appearance: light grey solid: LCMS: 1.72 min m/*z* 381.1, 383.1 ($(M + H)^+$ 1:1, $^{79/81}$Br), Purity>95%, Method D; ^{1}H NMR (500 MHz, DMSO-d_6) δ ppm 8.86 (s, 1 H), 7.39–7.30 (m, 4 H), 6.54 (d, J = 6.87 Hz, 1 H), 4.20 (ddd, J = 10.31, 8.59, 6.87 Hz, 1 H), 3.84 (ddd, J = 16.04, 12.03, 4.01 Hz, 1 H), 3.29–3.23 (m, 1 H), 3.18 (td, J = 9.45, 6.87 Hz, 1 H), 3.07–3.00 (m, 2 H), 2.66–2.56 (m, 2 H), 2.38–2.31 (m, 1 H), 1.75–1.67 (m, 1 H), 1.67–1.58 (m, 1 H), 1.57–1.46 (m, 3 H); ^{13}C NMR (126 MHz, CD_3OD) δ ppm 174.9, 157.8, 140.5, 133.0, 122.1, 115.9, 54.0, 51.3, 46.3, 41.5, 30.1, 28.5; HRMS: Exact Mass: 380.0848; $(M + H)^+$: 381.0928; Observed Mass: 381.0924; 1.05 ppm.

4.2.4.2. 1-(4-Bromophenyl)-3-[2-oxo-1-(4-piperidylmethyl)pyrrolidin-3-yl]urea (12). Compound was prepared according to general procedure D with intermediate: *tert*-butyl 4-[[3-[(4-bromophenyl) carbamoylamino]-2-oxo-pyrrolidin-1-yl]methyl] piperidine-1-carboxylate (**11**) (0.303 mmol). A crude product was dissolved in methanol. Methanol solution was passed through the Isolute NH2

SPE cartridge and filtrate was concentrated under reduced pressure to give the desired product as a free base. Yield: 120 mg, 100%; Appearance: light brown solid; LCMS: 1.75 min m/z 395.1, 397.1 ((M + H)$^+$ 1:1, $^{79/81}$Br), Purity>95%, Method D; ^{1}H NMR (500 MHz, CD_3OD) δ ppm 7.38–7.35 (m, 2 H). 7.33–7.28 (m, 2 H), 4.35 (t, J = 9.74 Hz, 1 H), 3.47–3.42 (m, 2 H), 3.28–3.21 (m, 4 H), 2.81 (td,J = 10.30, 2.86 Hz, 2 H), 2.52–2.44 (m, 1 H), 2.09–2.00 (m, 1 H), 2.00–1.90 (m, 1 H), 1.90–1.76 (m, 2 H), 1.38–1.27 (m, 2 H); ^{13}C NMR (126 MHz, CD_3OD) δ ppm 175.6, 157.5, 140.3, 132.8, 122.0, 115.8, 53.6, 50.2, 46.2, 45.7, 34.2, 29.2, 27.9; HRMS: Exact Mass: 394.1004; (M + H)$^+$: 395.1084; Observed Mass: 395.1081; 0.76 ppm.

4.2.4.3. 1-(4-Bromophenyl)-3-(2-oxo-1-pyrrolidin-3-yl-pyrrolidin-3-yl)urea (68). Compound was prepared according to general procedure D with intermediate *tert*-butyl 3-[3-[(4-bromophenyl)carbamoylamino]-2-oxo-pyrrolidin-1-yl] pyrrolidine-1-carboxylate (66) (0.16 mmol); A crude product was dissolved in methanol. Methanol solution was passed through the Isolute NH_2 SPE cartridge (500 mg) and filtrate was concentrated under reduced pressure to give the desired product as a free base. Yield: 59 mg, 100%; Appearance: light brown solid; LCMS: 1.69 min m/z 367.1, 369.1 ((M + H)$^+$ 1:1, $^{79/81}$Br), Purity = 90%, Method D; ^{1}H NMR (500 MHz, CD_3OD) δ ppm 7.37–7.33 (m, 2 H), 7.31–7.26 (m, 2 H), 4.55–4.46 (m, 1 H), 4.34 (t, J = 9.45 Hz, 1 H), 3.48–3.36 (m, 2 H), 3.14–3.03 (m, 2 H), 2.98–2.89 (m, 2 H), 2.51–2.44 (m, 1 H), 2.13–2.00 (m, 1 H), 1.98–1.86 (m, 2 H); ^{13}C NMR (126 MHz, CD_3OD) δ ppm 175.3, 157.6, 140.3, 132.8, 121.9, 115.7, 54.7, 53.7, 49.9, 47.2, 42.7, 30.3, 28.2.

4.2.4.4. 1-(4-Bromophenyl)-3-(2-oxo-1-pyrrolidin-3-yl-pyrrolidin-3-yl)urea (69). Compound was prepared according to general procedure D with intermediate *tert*-butyl 3-[3-[(4-bromophenyl)carbamoylamino]-2-oxo-pyrrolidin-1-yl] pyrrolidine-1-carboxylate (**67**) (0.1 mmol). A crude product was dissolved in methanol. Methanol solution was passed through the Isolute NH_2 SPE cartridge (500 mg) and tr filtrate was concentrated under reduced pressure to afford the desired product as a free base. Yield: 29 mg, 70%; Appearance: white solid; LCMS: 1.68 min m/z 367.0, 369.0 ((M + H)$^+$ 1:1, $^{79/81}$Br), Purity = 85%, Method D; ^{1}H NMR (500 MHz, CD_3OD) δ ppm 7.36–7.26 (m, 4 H), 4.56–4.46 (m, 1 H), 4.35 (dd, J = 10.31, 8.59 Hz, 1 H), 3.47–3.35 (m, 2 H), 3.11–2.97 (m, 2 H), 2.95–2.82 (m, 2 H), 2.51–2.43 (m, 1 H), 2.09–1.96 (m, 1 H), 1.95–1.83 (m, 2 H); ^{13}C NMR (126 MHz, CD_3OD) δ ppm 175.0, 157.4, 140.2, 132.7, 121.8, 115. 6, 54.3 53.5, 49.9, 47.1, 42.1, 29.8, 28.0.

4.2.5. General procedure E: N-alkylation

1-(4-bromophenyl)-3-[2-oxo-1-(4-piperidylmethyl)pyrrolidin-3-yl]urea (1 eq.) was dissolved in N,N-dimethylformamide (1 mL). To the reaction, N,N-diisopropylethylamine (0.1 mmol, 2 eq.) following benzyl bromide (1.1 eq.) were added via syringe. The reaction was stirred overnight. The crude product was purified by preparative HPLC under basic conditions to give final compound.

4.2.5.1. 1-[1-[(1-Benzyl-4-piperidyl)methyl]-2-oxo-pyrrolidin-3-yl]-3-(4-bromophenyl)urea (15). Compound was prepared according to general procedure P with intermediate 1-(4-bromophenyl)-3-[2-oxo-1-(4-piperidylmethyl)pyrrolidin-3-yl]urea (**12**) and benzyl bromide (1.2 equiv., 1 mmol). Yield: 10 mg, 30%; Appearance: white solid; LCMS: 2.18 min m/z 485.1, 487.1, ((M + H)$^+$ 1:1, $^{79/81}$Br), Purity = 95%, Method D; ^{1}H NMR (500 MHz, DMSO-d_6) δ ppm 8.74 (s, 1 H), 7.37–7.30 (m, 4 H), 7.30–7.22 (m, 4 H), 7.22–7.18 (m, 1 H), 6.47 (d, J = 6.87 Hz, 1 H), 4.22 (ddd, J = 10.31, 8.59, 6.87 Hz, 1 H), 3.41 (s, 2 H), 3.28–3.21 (m, 2 H), 3.05 (qd, J = 13.65, 7.16 Hz, 2 H), 2.73 (d, J = 10.88 Hz, 2 H), 2.37–2.30 (m, 1 H), 1.90–1.81 (m, 2 H), 1.81–1.70 (m, 1 H), 1.59–1.46 (m, 3 H), 1.15–1.03 (m, 2 H); ^{13}C NMR (126 MHz, DMSO-d_6) δ ppm 172.2, 154.8, 139.7, 138.6, 131.4, 128.7, 128.1, 126.8, 119.6, 112.5, 62.3, 52.7, 51.1, 48.0, 43.9, 33.6, 29.5, 27.5; HRMS: Exact mass: 484.1474; (M + H)$^+$: 485.1554; Observed mass: 485.1545; 1.86 ppm.

4.2.5.2. 1-[1-(1-Benzyl-4-piperidyl)-2-oxo-pyrrolidin-3-yl]-3-(4-bromophenyl)urea (16). Compound was prepared according to general procedure P with intermediate: 1-(4-bromophenyl)-3-[2-oxo-1-(4-piperidyl)pyrrolidin-3-yl]urea (**13**) (0.066 mmol) and benzyl bromide (1.2 equiv., 0.9 mmol). Crude product was purified by prep. HPLC (19 × 100mm (5 μm) C-18 Waters Xbridge, MeOH pH = 10). Yield: 10 mg, 30%; Appearance: white solid; LCMS: 2.184 min m/z 471.1, 473.1 ((M + H)$^+$ 1:1, $^{79/81}$Br), Purity = 95%, Method D; ^{1}H NMR (500 MHz, DMSO-d_6) δ ppm 8.75 (s, 1 H), 7.36–7.20 (m, 9H), 6.48 (d, J = 6.87 Hz, 1 H), 4.19 (ddd, J = 5.16, 6.87, 10.31 Hz, 1 H), 3.70 (tt, J = 4.08, 11.96 Hz, 1 H), 3.42 (s, 2 H), 3.29 (d, J = 9.16 Hz, 1H), 3.18 (dt, J = 2.86, 6.30 Hz, 1 H), 3.14–3.13 (m, 1 H), 2.86–2.78 (m, 2 H), 2.37–2.30 (m, 1 H), 1.96 (dd, J = 2.29, 11.46 Hz, 2 H), 1.74–1.60 (m, 3 H), 1.53–1.42 (m, 2 H); HRMS: Exact mass: 470.1317; (M + H)$^+$: 471.1397; Observed mass: 471.1395; 0.43 ppm.

4.2.5.3. 1-[1-(1-Benzylpyrrolidin-3-yl)-2-oxo-pyrrolidin-3-yl]-3-(4-bromophenyl)urea (17). Compound was prepared according to general procedure P with intermediate 1-(4-bromophenyl)-3-(2-oxo-1-pyrrolidin-3-yl-pyrrolidin-3-yl)urea (**68**) (0.08 mmol) and benzyl bromide (1.2 equiv., 1 mmol). Crude product was purified by prep. HPLC (19 × 100mm (5 μm) C-18 Waters Xbridge, MeOH pH = 10). Yield: 16 mg, 40%; Appearance: white solid; LCMS: 2.194 min m/z 457, 459 ((M + H)$^+$ 1:1, $^{79/81}$Br), Purity = 95%, Method D; ^{1}H NMR (500 MHz, DMSO-d_6) δ ppm 8.95–8.82 (br.s, 1 H), 7.55–7.43 (m, 5 H), 7.41–7.34 (m, 5 H), 6.70–6.56 (br.s, 1 H), 4.80–4.60 (m, 1 H), 4.52–4.36 (m, 1 H), 4.36–4.16 (m, 2 H), 3.53–3.39 (m, 2 H), 3.30–3.16 (m, 2 H), 2.45–2.25 (m, 2 H), 2.22–1.95 (m, 2 H), 1.94–1.63 (m, 2 H); broad peaks due to presence of rotamers. HRMS: Exact mass: 456.1161; (M + H)$^+$: 457.1241; Observed mass: 457.1238; 0.66 ppm.

4.2.5.4. 1-[1-(1-Benzylpyrrolidin-3-yl)-2-oxo-pyrrolidin-3-yl]-3-(4-bromophenyl)urea (18). Compound was prepared according to general procedure G with intermediate 1-(4-bromophenyl)-3-(2-oxo-1-pyrrolidin-3-yl-pyrrolidin-3-yl)urea (**69**); Crude product was purified by prep. HPLC (19 × 100mm (5 μm) C-18 Waters Xbridge, MeOH pH = 10); Yield: 12 mg, 30%; Appearance: white solid; LCMS: 2.198 min, m/z 457, 459 ((M + H)$^+$ 1:1, $^{79/81}$Br), Purity = 95%, Method D; ^{1}H NMR (500 MHz, DMSO-d_6) δ ppm 8.97–8.80 (br.s, 1 H), 7.40–7.29 (m, 9 H), 6.66–6.51 (br.s, 1 H), 4.65–4.40 (m, 1 H), 4.49–4.30 (m, 1 H), 4.29–4.15 (m, 2 H), 3.48–3.34 (m, 2 H), 3.27–3.12 (m, 2 H), 2.39–2.26 (m, 2 H), 2.14–1.94 (m, 2 H), 1.85–1.68 (m, 2 H); broad peaks due to presence of rotamers; HRMS: Exact mass: 456.1161; (M + H)$^+$: 457.1241; Observed mass: 457.1238; 0.66 ppm.

4.3. General biological procedures

4.3.1. Culture of CHO–K1 FPRL1 cells

PathHunter® CHO–K1 FPRL1 cells (DISCOVERx) were grown in the F-12 nutrient mixture (HAM) (21765–037, Gibco®) supplemented with 10% Fetal Bovine Serum (A3840401, Thermo Fisher Sci), Hygromycin B 800 μg/mL (10687–010, Thermo Fisher Sci), Geneticin 300 μg/mL (10131–027, Thermo Fisher Sci). The cells were incubated at 37 °C and passaged every 2–3 days, based on the doubling time of the cell line. The Accutase ® (AT104-500) was used as the cell detachment solution.

4.3.2. β-Arrestin path Hunter® assay detection protocol

To identify novel FPR2 agonists PathHunter® CHO−K1 FPRL1 cells (DISCOVERx) expressing complementing fragments of the β-galactosidase (β-gal) enzyme were used. One day before the assay, the cells were diluted to a concentration of 0.5 x 10^6/mL in DISCOVERx plating media (Assay CompleteTM Cell Plating 2 Reagent; 93−0563R2A). The cells were plated out 10 μL per well of 384 well plate (5000 cells per well) and incubated 1 h at room temperature then overnight at 37 °C. 10 mM stock solutions of compounds were serially diluted in assay buffer (PBS using a half log dilution protocol on a Biomek instrument (automated liquid handler). The compound addition to the assay plate was performed Biomek instrument. Cells were stimulated with compounds or for high controls with W-peptide (a control ligand sequence WKYMVm; concentration = 100 nM) for 150 min at 37 °C. Detection reagent (19 parts Assay buffer, 5 parts Emerald II and 1 part Galacton Star; Pathhunter detection kit (93−0001) DISCOVERx) was added 12 μL per well and incubated for 60 min in the dark at room temperature. Receptor activation was determined by chemiluminescence using a BMG Pherastar plate reader. Raw data were entered into GraphPad Prism 7.01 analysis software for data processing and visualisation.

4.3.3. Calcium mobilization assay protocol

The increase in cytosolic Ca^{2+} was measured by the FLIPR® Tetra® High-Throughput Cellular Screening System. In the calcium mobilization assay FLIPR calcium 6 dye (Molecular Devices) was used. One day before the assay, the cells were diluted to a concentration of 0.5 × 10^6/mL in F-12 nutrient mixture (HAM) (21765−037, Gibco®) containing 10% Fetal Bovine Serum (A3840401, Thermo Fisher Sci) and plated out 40 μL per well of 384 well plate (20,000 cells per well) then incubated 1 h at RT and then overnight at 37 °C. On the assay day, media was removed from the cell plate and 20 μLs of dye per well were added. The cell plate was incubated for 2 h at 37 °C and later for 30 min at RT in the dark. 10 mM stock solutions of compounds were serially diluted in assay buffer (HBSS 20 mM HEPES) using a half log dilution protocol on a Biomek instrument (automated liquid handler). In both assays W-peptide was used as a control compound (100 nM). The 5 μL compound addition was performed by the FLIPR® Tetra® High-Throughput Cellular Screening System. The calcium mobilization was measured for 240s (Read Mode: Exc. Wavelength 470−495 nm, Em. Wavelength 515−575 nm, Gain: 2000). Data are processed using ScreenWorks 4.0.0.30. Raw data were entered into GraphPad Prism 7.01 analysis software for data processing and visualisation.

4.3.4. Isolation of human neutrophils from venous blood

Blood was collected from healthy donors in accordance with a protocol approved by the Ludwig Maximilian University of Munich. Neutrophils were isolated from the blood using Polymorphprep (Axi-Shield) following the manufacturer's instructions. Isolated neutrophils were washed and resuspended in HBSS buffer containing 20 mM HEPES, 0.25% BSA, Ca^{2+} pH 7.4 (0.5 × 10^6 cells/mL) and used on the day of the experiment.

4.3.5. Human neutrophil static adhesion assay

The static adhesion assay was performed with the aim of examining the small molecule agonists and their anti-inflammatory and proresolving properties. The day before the assay, 96-well flat-bottomed plates were coated with 50 μL of cell adhesion molecules, both with a final concentration of 1 μg/mL: P-selectin (13025-H02H-100; SinoBiological) and ICAM- 1 (10346-H03H-100; SinoBiological). The coated plates were kept at 40 °C overnight. The excess of solution was removed with pipette and the unspecific binding was blocked with BSA 2% for 1 h at room temperature. Per well of the pre-incubation plate, 120 μL of neutrophils (0.5 × 10^6 cells/mL) and 30 μL of the agonists (final dilution 1:5) were added. Cells were incubated 30 min 37 °C with gentle continuous mixing. From the pre-incubation plate, 125 μL of the reaction mixture was transferred into the pre-coated assay plate, followed by an incubation of 20 min at 37 °C. Non-adherent neutrophils were removed, and the fixation step was performed with PFA 4%. Cells were stained with DAPI for 10 min and then washed gently with 200 μL PBS. Four pictures per well were taken with a Leica microscope (DMI8, software: LAS X. V.3.4.2.18368, autofocus, exposure 51−57 ms, gain: 1.5, DAPI). The image files were processed using an ImageJ macro. Raw data were entered into GraphPad Prism 7.01 analysis software for data processing and visualisation. Each compound was tested in technical triplicates.

4.3.6. Cell culture and ERK1/2 assay

HEK293A cells and FPR1 or FPR2 stably transfected HEK293A cells were maintained in DMEM containing 10% FCS and 1% penicillin/streptomycin and kept at 37 °C with 5% CO_2. Cells were seeded in 96-wells plates at 2 × 10^4 cells/well and allow to grow for 48 h.

4.3.7. ERK phosphorylation assay

Cells were serum-starved for 3 h to stabilize basal levels of signalling and reduce background levels of p-ERK. Drug solutions were prepared in 0% FCS DMEM. Compounds were tested using 30 μM as top concentration followed by 1/3 serial dilutions to generate concentration response curves. Cells were stimulated for 5 min with drugs and lysed immediately with ice-cold extraction buffer supplied in the ERK1/2 (pT202/Y204) SimpleStep ELISA Kit (Abcam ab176640), used for p-ERK quantification according to manufacturer instructions. Optical Density (OD) measurements were converted to calculate relative p-ERK quantity and results were expressed as increment over basal levels for each receptor subtype.

4.3.8. Statistical data analysis

GraphPad Prism 7.01 (GraphPad Software, San Diego, CA, USA) was used for statistical analysis of the data. For comparison of treatment groups with the control group and P- value determination, the one-way ANOVA analysis followed by Dunnett's multiple comparison test was used. All data were shown as means ± SEM. Differences were considered statistically significant for a $P < 0.05$. P value; ***$P < 0.001$; **$P < 0.01$; *$P < 0.05$, ns − nonsignificant.

4.3.9. PK studies

The pharmacokinetic studies were performed in male C57BL6 mice with intraperitoneal administration at 10 mg/kg. In total 12 mice were used: 9 received the compound and 3 mice for blank plasma collection for bioanalysis. Compound concentration in plasma was measured at eight time points over 24 h. Each mouse used in the study was bled thrice with sufficient time gap. Mice (n = 12) were treated with either the vehicle (DMSO (10%) + PEG400 (35%) + PG (25%) + water (30%)) or a clear solution of Compound 7 (10 mg/kg in vehicle).

4.3.10. Cell health assay

In order to measure a variety of parameters which leads to cell viability, cell death, cytotoxicity or cell proliferation, the cell health assay was performed. A human hepatocyte carcinoma cells (HepG2 cells EACC origin) were cultured a week before assay in Eagle's Minimum Essential Medium (EMEM) inc. NEAA (non-essential amino acids) with 10% Fetal Bovine Serum and 2 mM GlutaMAX. During cell plating 1% Penicillin/Streptomyocin was added to media. 2000 HepG2 cells per well were plated in 25 μL media of a 384 well plate and incubated at 37 °C overnight. The compounds were

added from the serial dilution plates using Biomek robot (automated liquid handler). The assay plates were incubated at 37 °C for 72 h. Four live staining dyes were added on Biomek robot and plates were incubate 1 h at 37 °C. Cell measurements were imaged on the InCELL Analyzer 2000 using the following four wavelength channels for each of the four dyes: Hoechst (nuclei) - DAPI channel; Fluo-4 AM (cellular calcium) - Fluorescein isothiocyanate (FITC) channel; Tetramethylrhodamine, methyl ester (TMRM) (mitochondria) - Texas Red channel; TOTO-3 (dead nuclei) – Cy® 5 channel. Raw data were processed and visualized in Genedata Screener analysis software. The cell measurements were normalised as a percentage in contradiction of low control. Any cell parameter that deviates from 100% baseline shows a variation in cell phenotype and cytotoxicity after drug treatment.

4.3.11. Kinetic solubility measurements

The kinetic solubility was measured by diluting a 4 μL of 10 mM DMSO stock solution of the compound into PBS buffer pH 7.4 in a filtration plate at a target concentration of 200 μM giving a final solution composition of 98:2 PBS:DMSO. For each compound, measurements were performed in triplicates with two standard compounds (Verapamil and Ketoconazole) on the same plate. The filtration plate was agitated at 500 rpm for 90 min and then filtered into V-bottom plate. The filtrate was sampled and diluted further with a DMSO:PBS mixture in a flat bottomed UV plate resulting with a final solution composition of PBS:DMSO 80:20. A serial dilution for each compound was then performed in flat bottomed plates in PBS:DMSO 80:20 with concentrations 200 μM, 100 μM, 50 μM, 25 μM, 12.5 μM and 6.75 μM. The UV absorbance was read across 230–400 nm at 1 nm intervals using a TECAN Safire II plate reader and a suitable UV wavelength chosen around the UV maximum of each compound. This was used to calculate the concentration in the filtrate for each compound, and hence amount remaining in solution after 90 min which is reported as the kinetic solubility.

4.3.12. LogD measurements

LogD measurements were conducted using the shake flask method. Compound was diluted from 10 mM DMSO stock solution into an Eppendorf containing equal amounts of octanol and phosphate buffered saline (PBS) to give a final concentration of 100 μM. The tubes were shaken for 12 h, centrifuged at 10000 rpm for 10 min and samples taken from the octanol and PBS layers. The samples from both layers were analysed in triplicate by LC-MS/MS (Agilent Technologies G6410 series, triple quadrupole with MM-ESI ion source) using optimised multiple reaction monitoring (MRM) scans and a standard column gradient on an Acquity UPLC BEH C8 1.7 μm column, running acetonitrile and water with 0.05% Acetic Acid as the mobile phase. The ratios of areas of the peaks were used to calculate the LogD in accordance with the equation: LogD = Log10(Area-TL/Area BL).

4.3.13. Microsomal stability assay

The human and mouse liver microsomes (MLM) were obtained from BD Biosciences. The compounds were pre-incubated at 37 °C for 5 min with the microsomes and the reaction was initiated by adding an equal volume of NADPH generating solution (BD Biosciences). The final compound concentration in the incubation is 1 μM, and the microsomal protein concentration is 0.2 mg/mL. A sample was taken at t = 0 and quenched with two times volume of ice-cold methanol containing an internal standard reference compound (Carbamazepine). The reaction was agitated at 37 °C for 30 min, when a further sample was taken and quenched in an identical fashion. The samples were centrifuged at 10000 rpm for 10 min and the supernatant taken for analysis in triplicate by LC-MS/MS (Agilent Technologies G6410 series, triple quadrupole with MM-ESI ion source) using optimised multiple reaction monitoring scans and a standard column gradient on an Acquity UPLC BEH C8 1.7 μm column (mobile phase: acetonitrile and water with 0.05% acetic). The % turnover was obtained by calculating the percentage difference of the peak areas, normalised to the internal standard, at t = 0 and t = 30. Verapamil was used as the standard compound.

Contributors

TC supervised the findings of this work and conceived the studies. OS conceived and designed the neutrophil studies. AM was involved in planning and supervised the work. MP is the Coordinator of the Marie Skłodowska-Curie ITN EVOluTION and was involved in supervision the work. MM performed *in silico* studies, designed and synthesized the compounds, performed and analysed the *in vitro* assays. GN supervised the *in-silico* studies. MM performed and analysed the human neutrophil static assays and contributed to all the stages of the experimental work. AOG and MM designed the human neutrophil static adhesion assay. SM aided in interpreting the results. SM and BF performed *in vivo* studies. JGM performed and analysed the ERK phosphorylation assay. MM and TC prepared the first draft of the manuscript. All authors have given approval to the final version of the manuscript.

Declaration of competing interest

The authors declare the following financial interests/personal relationships which may be considered as potential competing interests: MP is shareholder of ResoTher Pharma which is developing FPR2 peptide-agonists for clinical application. MM, TC, OS, AM, GN, AOG, BF, JGM and SM declare that they have no known competing financial interests or personal relationships that could have appeared to influence the work reported in this paper.

Acknowledgment

The authors would like to acknowledge Dr David Tickle, Teresa Sementa and Sadhia Khan for performing the *in vitro* ADME testing. We are grateful to Anthony Weatherhead for carrying out the HRMS measurements, to Nathalie Bouloc for her assistance in preparative HPLC purification of the compounds and to Michelle Newman for performing the cell health assay. We would also like to thank Dr Kris Birchall for his assistance with the *in silico* studies.

Abbreviations

ACN	Acetonitrile
ADME	Absorption, Distribution, Metabolism, Excretion
BOC	*tert*-Butyloxycarbonyl
BSA	Bovine Serum Albumin
CL_{int}	Intrinsic Clearance
CVDs	Cardiovascular Diseases
DAPI	4′,6-Diamidino-2-phenylindole
DCC	*N*,*N*′-Dicyclohexylcarbodiimide
DCM	Dichloromethane
DCE	Dichloroethane
DIPEA	*N*,*N*-Diisopropylethylamine
DMAP	4-Dimethylaminopyridine
DMF	*N*,*N*–Dimethylformamide
DMSO	Dimethyl Sulfoxide
EC_{50}	Half Maximal Effective Concentration
E_{max}	Efficacy
FPR2	Formyl Peptide Receptor 2

GLASS database	GPCR-Ligand Association database
GPCR	G-Protein-Coupled Receptors
HBSS	Hanks' Balanced Salt Solution
HEPES	4-(2-Hydroxyethyl)-1-Piperazineethanesulfonic Acid
HLM	Human Liver Microsomes
HPLC	High Performance Liquid Chromatography
HRMS	High Resolution Mass Spectrometry
ICAM	Intercellular Adhesion Molecule
Ks	Kinetic Solubility
LC-MS	Liquid Chromatography-Mass Spectroscopy
LogD	Logarithm of Distribution-Coefficient
MLM	Mouse Liver Microsomes
NA	No Activity
NMR	Nuclear Magnetic Resonance
ON	Overnight
PE	Petroleum Ether
PFA	Paraformaldehyde
PK	Pharmacokinetics
RoI	Resolution of Inflammation
ROC	Receiver Operating Characteristic
SAA	Serum Amyloid A
SAR	Structure-Activity Relationship
TEA	Triethylamine
TM	Template Model
T3P	Propylphosphonic Anhydride
THF	Tetrahydrofuran
VCAM	Vascular Cell Adhesion Molecule

Appendix A. Supplementary data

Supplementary data to this article can be found online at https://doi.org/10.1016/j.ejmech.2021.113805.

Funding

This work was supported by the European Union's Horizon 2020 research and innovation program under the Marie Sklodowska-Curie grant agreement No. 675111.

References

[1] M.H. Petri, A. Laguna-Fernandez, M. Gonzalez-Diez, G. Paulsson-Berne, G.K. Hansson, M. Back, The role of the FPR2/ALX receptor in atherosclerosis development and plaque stability, Cardiovasc. Res. 105 (1) (2015) 65–74.
[2] N.E. Kieran, P.P. Doran, S.B. Connolly, M.C. Greenan, D.F. Higgins, M. Leonard, C. Godson, C.T. Taylor, A. Henger, M. Kretzler, M.J. Burne, H. Rabb, H.R. Brady, Modification of the transcriptomic response to renal ischemia/reperfusion injury by lipoxin analog, Kidney Int. 64 (2) (2003) 480–492.
[3] G. Leoni, O. Soehnlein, (Re) solving repair after myocardial infarction, Front. Pharmacol. 9 (2018), 1342-1342.
[4] R.A. García, B.R. Ito, J.A. Lupisella, N.A. Carson, M.-Y. Hsu, G. Fernando, M. Heroux, M. Bouvier, E. Dierks, E.K. Kick, D.A. Gordon, J. Chen, G. Mintier, M. Carrier, S. St-Onge, H. Shah, J. Towne, M.S. Bucardo, X. Ma, C.S. Ryan, N.R. Wurtz, J. Ostrowski, F.J. Villarreal, Preservation of post-infarction cardiac structure and function via long-term oral formyl peptide receptor agonist treatment, J Am Coll Cardiol Basic Trans Science 349 (2019).
[5] B.E. Sansbury, M. Spite, Resolution of acute inflammation and the role of resolvins in immunity, thrombosis, and vascular biology, Circ. Res. 119 (1) (2016) 113–130.
[6] M. Arita, T. Ohira, Y.P. Sun, S. Elangovan, N. Chiang, C.N. Serhan, Resolvin E1 selectively interacts with leukotriene B4 receptor BLT1 and ChemR23 to regulate inflammation, J. Immunol. 178 (6) (2007) 3912–3917.
[7] C.B. Clish, K. Gronert, C.N. Serhan, Local and systemic delivery of an aspirin-triggered lipoxin stable analog inhibits neutrophil trafficking, Ann. N. Y. Acad. Sci. 905 (2000) 274–278.
[8] C.B. Clish, J.A. O'Brien, K. Gronert, G.L. Stahl, N.A. Petasis, C.N. Serhan, Local and systemic delivery of a stable aspirin-triggered lipoxin prevents neutrophil recruitment in vivo, Proc. Natl. Acad. Sci. U. S. A. 96 (14) (1999) 8247–8252.
[9] V. Kain, J.K. Jadapalli, B. Tourki, G.V. Halade, Inhibition of FPR2 impaired leukocytes recruitment and elicited non-resolving inflammation in acute heart failure, Pharmacol. Res. 146 (2019) 104295.
[10] C.N. Serhan, J.F. Maddox, N.A. Petasis, I. Akritopoulou-Zanze, A. Papayianni, H.R. Brady, S.P. Colgan, J.L. Madara, Design of lipoxin A4 stable analogs that block transmigration and adhesion of human neutrophils, Biochemistry 34 (44) (1995) 14609–14615.
[11] M.A. Sugimoto, J.P. Vago, M.M. Teixeira, L.P. Sousa, Annexin A1 and the resolution of inflammation: modulation of neutrophil recruitment, apoptosis, and clearance, J Immunol Res 2016 (2016) 8239258.
[12] J.F. Maddox, M. Hachicha, T. Takano, N.A. Petasis, V.V. Fokin, C.N. Serhan, Lipoxin A4 stable analogs are potent mimetics that stimulate human monocytes and THP-1 cells via a G-protein-linked lipoxin A4 receptor, J. Biol. Chem. 272 (11) (1997) 6972–6978.
[13] M. Perretti, C. Godson, Formyl peptide receptor type 2 agonists to kick-start resolution pharmacology, Br. J. Pharmacol. 177 (20) (2020) 4595–4600.
[14] M. Perretti, X. Leroy, E.J. Bland, T. Montero-Melendez, Resolution pharmacology: opportunities for therapeutic innovation in inflammation, Trends Pharmacol. Sci. 36 (11) (2015) 737–755.
[15] M.A. Sugimoto, L.P. Sousa, V. Pinho, M. Perretti, M.M. Teixeira, Resolution of inflammation: what controls its onset? Front. Immunol. 7 (2016).
[16] Y. Zhuang, H. Liu, X. Edward Zhou, R. Kumar Verma, P.W. de Waal, W. Jang, T.H. Xu, L. Wang, X. Meng, G. Zhao, Y. Kang, K. Melcher, H. Fan, N.A. Lambert, H. Eric Xu, C. Zhang, Structure of formylpeptide receptor 2-Gi complex reveals insights into ligand recognition and signaling, Nat. Commun. 11 (1) (2020) 885.
[17] H.Q. He, R.D. Ye, The formyl peptide receptors: diversity of ligands and mechanism for recognition, Molecules 22 (3) (2017).
[18] S. Bozinovski, D. Anthony, R. Vlahos, Targeting pro-resolution pathways to combat chronic inflammation in COPD, J. Thorac. Dis. 6 (11) (2014) 1548–1556.
[19] Y. Asahina, N.R. Wurtz, K. Arakawa, N. Carson, K. Fujii, K. Fukuchi, R. Garcia, M.Y. Hsu, J. Ishiyama, B. Ito, E. Kick, J. Lupisella, S. Matsushima, K. Ohata, J. Ostrowski, Y. Saito, K. Tsuda, F. Villarreal, H. Yamada, T. Yamaoka, R. Wexler, D. Gordon, Y. Kohno, Discovery of BMS-986235/LAR-1219: a potent formyl peptide receptor 2 (FPR2) selective agonist for the prevention of heart failure, J. Med. Chem. 63 (17) (2020) 9003–9019.
[20] A.K. Stalder, D. Lott, D.S. Strasser, H.G. Cruz, A. Krause, P.M. Groenen, J. Dingemanse, Biomarker-guided clinical development of the first-in-class anti-inflammatory FPR2/ALX agonist ACT-389949, Br. J. Clin. Pharmacol. 83 (3) (2017) 476–486.
[21] O. Corminboeuf, X. Leroy, FPR2/ALXR agonists and the resolution of inflammation, J. Med. Chem. 58 (2) (2015) 537–559.
[22] M. Maciuszek, A. Cacace, E. Brennan, C. Godson, T.M. Chapman, Recent advances in the design and development of formyl peptide receptor 2 (FPR2/ALX) agonists as pro-resolving agents with diverse therapeutic potential, Eur. J. Med. Chem. 213 (2021) 113167.
[23] A.J. Kooistra, S. Mordalski, G. Pándy-Szekeres, M. Esguerra, A. Mamyrbekov, C. Munk, G.M. Keserű, D.E. Gloriam, GPCRdb in 2021: integrating GPCR sequence, structure and function, Nucleic Acids Res. 49 (D1) (2021) D335–D343.
[24] G. Pándy-Szekeres, C. Munk, T.M. Tsonkov, S. Mordalski, K. Harpsøe, A.S. Hauser, A.J. Bojarski, D.E. Gloriam, GPCRdb, Adding GPCR structure models and ligands, Nucleic Acids Res., **2018** 46 (D1) (2018) D440–D446.
[25] T. Wang, Z. Li, M. Cvijic, C. Krause, L. Zhang, C. Sum, Measurement of β-Arrestin Recruitment for GPCR Targets, 2019.
[26] P.Y. Jean-Charles, S. Kaur, S.K. Shenoy, G, Protein-coupled receptor signaling through β-arrestin-dependent mechanisms, J. Cardiovasc. Pharmacol. 70 (3) (2017) 142–158.
[27] M. Qiang, Y. Lingyan, L. Hongxia, S. Ying, Z. Naiming, An overview of Ca^{2+} mobilization assays in GPCR drug discovery, Expet Opin. Drug Discov. 12 (5) (2017) 511–523.
[28] B.K. Kobilka, G, Protein coupled receptor structure and activation, Biochim. Biophys. Acta 1768 (4) (2007) 794–807.
[29] E.J. Whalen, S. Rajagopal, R.J. Lefkowitz, Therapeutic potential of β-arrestin- and G protein-biased agonists, Trends Mol. Med. 17 (3) (2011) 126–139.
[30] J.S. Smith, T.F. Pack, A. Inoue, C. Lee, K. Zheng, I. Choi, D.S. Eiger, A. Warman, X. Xiong, Z. Ma, G. Viswanathan, I.M. Levitan, L.K. Rochelle, D.P. Staus, J.C. Snyder, A.W. Kahsai, M.G. Caron, S. Rajagopal, Noncanonical scaffolding of G αi and β-arrestin by G protein-coupled receptors, Science 371 (6534) (2021), eaay1833.
[31] C.A. Raabe, J. Gröper, U. Rescher, Biased perspectives on formyl peptide receptors, Biochim. Biophys. Acta Mol. Cell Res. 1866 (2) (2019) 305–316.
[32] S. Gallo, A. Vitacolonna, A. Bonzano, P. Comoglio, T. Crepaldi, ERK: a key player in the pathophysiology of cardiac hypertrophy, Int. J. Mol. Sci. 20 (9) (2019) 2164.
[33] C.X. Qin, L.T. May, P.M. Sexton, A.J. DeBono, J.B. Baell, A. Christopoulos, R.H. Ritchie, Correspondence: reply to 'Compound 17b and formyl peptide receptor biased agonism in relation to cardioprotective effects in ischaemia-reperfusion injury', Nat. Commun. 9 (1) (2018) 530.
[34] C.X. Qin, L.T. May, R. Li, N. Cao, S. Rosli, M. Deo, A.E. Alexander, D. Horlock, J. Bourke, Y.H. Yang, A.G. Stewart, D.M. Kaye, X.-D. Du, P.M. Sexton, A. Christopoulos, X.-M. Gao, R.H. Ritchie, Small-molecule-biased formyl peptide receptor agonist compound 17b protects against myocardial ischaemia-reperfusion injury in mice, Nat. Commun. 8 (2017) 14232.
[35] W.K.B. Chan, H. Zhang, J. Yang, J.R. Brender, J. Hur, A. Özgür, Y. Zhang, GLASS: a comprehensive database for experimentally validated GPCR-ligand associations, Bioinformatics 31 (18) (2015) 3035–3042.
[36] M. Maciuszek, A. Ortega-Gomez, S.L. Maas, M. Perretti, A. Merritt,

O. Soehnlein, T.M. Chapman, Synthesis and evaluation of novel cyclopentane urea FPR2 agonists and their potential application in the treatment of cardiovascular inflammation, Eur. J. Med. Chem. 214 (2021) 113194.
[37] S.L. Dixon, A.M. Smondyrev, E.H. Knoll, S.N. Rao, D.E. Shaw, R.A. Friesner, PHASE: a new engine for pharmacophore perception, 3D QSAR model development, and 3D database screening: 1. Methodology and preliminary results, J. Comput. Aided Mol. Des. 20 (10) (2006) 647–671.
[38] J. Ansari, E.Y. Senchenkova, S.A. Vital, Z. Al-Yafeai, G. Kaur, E.M. Sparkenbaugh, A.W. Orr, R. Pawlinski, R.P. Hebbel, D.N. Granger, P. Kubes, F.N.E. Gavins, Targeting the AnxA1/Fpr2/ALX pathway regulates neutrophil function, promoting thromboinflammation resolution in sickle cell disease, Blood 137 (11) (2021) 1538–1549.
[39] F.N. Gavins, M.J. Hickey, Annexin A1 and the regulation of innate and adaptive immunity, Front. Immunol. 3 (2012) 354.
[40] H.K. Smith, C.D. Gil, S.M. Oliani, F.N. Gavins, Targeting formyl peptide receptor 2 reduces leukocyte-endothelial interactions in a murine model of stroke, FASEB J 29 (5) (2015) 2161–2171.
[41] R.A. Teixeira, K.K. Mimura, L.P. Araujo, K.V. Greco, S.M. Oliani, The essential role of annexin A1 mimetic peptide in the skin allograft survival, J Tissue Eng Regen Med 10 (2) (2016) E44–E53.
[42] A. Jovanovic, Cardioprotective signalling: past, present and future, Eur. J. Pharmacol. 833 (2018) 314–319.
[43] M. Ibrahim-Ouali, M.-E. Sinibaldi, Y. Troin, D. Gardette, J.-C. Gramain, Synthesis of β-enaminoesters and lactams by michael addition of N-benzylaniline to new allenic esters and lactams, Synth. Commun. 27 (11) (1997) 1827–1848.
[44] X. Lin, W. Chen, Z. Qiu, L. Guo, W. Zhu, W. Li, Z. Wang, W. Zhang, Z. Zhang, Y. Rong, M. Zhang, L. Yu, S. Zhong, R. Zhao, X. Wu, J.C. Wong, G. Tang, Design and synthesis of orally bioavailable aminopyrrolidinone histone deacetylase 6 inhibitors, J. Med. Chem. 58 (6) (2015) 2809–2820.